The Q_{Weak} Experiment at Jefferson Lab: Searching for TeV Scale Physics by Measuring the Weak Charge of the Proton

Or, why measuring part-per-billion asymmetries to percent-level accuracy is really hard...

Wouter Deconinck

William & Mary

Supported by the NSF under Grant Nos.
PHY-1206053 and PHY-1405857.

March 6, 2017
University of Tennessee, Knoxville

There are Two Main Classes of Standard Model Tests

Current status of the Standard Model

Standard Model is an effective low-energy theory of the more fundamental underlying physics.

Complementary approaches to uncover the underlying physics

- Energy frontier: direct searches for new particles
- Precision or intensity frontier: indirect searches

Energy frontier

- Highest energies
- Few signature events
- *E.g.*: Tevatron, LHC

Precision or intensity frontier

- Modest or low energies
- High statistical power
- $g-2$, EDM, $\beta\beta$, rare decays
- Fundamental symmetries

Section 1

Precision Electroweak Tests of the Standard Model

Electroweak Interaction: An Introduction

Glashow–Weinberg–Salam theory of weak interaction

- Gauge symmetry: $SU(2)_L \times U(1)_Y$
- Gauge couplings: g for $SU(2)_L$, g' for $U(1)_Y$
- Left-handed leptons in doublets, right-handed in singlets
- Fundamental symmetry of left and right is broken

Parity symmetry is violated

- Weak interaction violates parity
- Electromagnetism satisfies parity
- Use parity-violation to measure internal electroweak parameters

Electroweak Interaction: An Introduction

Glashow–Weinberg–Salam theory of weak interaction

- Gauge symmetry: $SU(2)_L \times U(1)_Y$
- Gauge couplings: g for $SU(2)_L$, g' for $U(1)_Y$
- Left-handed leptons in doublets, right-handed in singlets
- Fundamental symmetry of left and right is broken

Parity symmetry is violated

- Weak interaction violates parity
- Electromagnetism satisfies parity
- Use parity-violation to measure internal electroweak parameters

Electroweak Interaction: An Introduction

Glashow–Weinberg–Salam theory of weak interaction

- Gauge symmetry: $SU(2)_L \times U(1)_Y$
- Gauge couplings: g for $SU(2)_L$, g' for $U(1)_Y$
- Left-handed leptons in doublets, right-handed in singlets
- Fundamental symmetry of left and right is broken

Electroweak symmetry breaking ($B_\mu, W_\mu^i \to A_\mu, Z_\mu^0, W_\mu^\pm$)

- $A_\mu, Z_\mu^0, W_\mu^\pm$ are mixture of B_μ and W_μ^i
- Gauge field A_μ remains massless (photon)
- Gauge fields $Z_\mu^0, W_\mu^\pm$ obtain mass (weak bosons)
- Weinberg angle θ_W describes how they mix

Electroweak Interaction: An Introduction

Glashow–Weinberg–Salam theory of weak interaction

- Gauge symmetry: $SU(2)_L \times U(1)_Y$
- Gauge couplings: g for $SU(2)_L$, g' for $U(1)_Y$
- Left-handed leptons in doublets, right-handed in singlets
- Fundamental symmetry of left and right is broken

Electroweak symmetry breaking $(B_\mu, W_\mu^i \to A_\mu, Z_\mu^0, W_\mu^\pm)$

$$\sin^2\theta_W = \frac{g'^2}{g^2 + g'^2} = 0.23122 \pm 0.00015\,(\text{at } M_Z) \approx \frac{1}{4}$$

$$\begin{aligned}
A_\mu &= \cos\theta_W \cdot B_\mu + \sin\theta_W \cdot W_\mu^3 && (\text{massless}) \\
Z_\mu^0 &= -\sin\theta_W \cdot B_\mu + \cos\theta_W \cdot W_\mu^3 && (M_Z \approx 91.2\,\text{GeV}) \\
W_\mu^\pm &= (W_\mu^1 \mp i W_\mu^2)/\sqrt{2} && (M_W \approx 80.4\,\text{GeV})
\end{aligned}$$

Electroweak Interaction: An Introduction

Glashow–Weinberg–Salam theory of weak interaction

- Gauge symmetry: $SU(2)_L \times U(1)_Y$
- Gauge couplings: g for $SU(2)_L$, g' for $U(1)_Y$
- Left-handed leptons in doublets, right-handed in singlets
- Fundamental symmetry of left and right is broken

Parity-violation neutral current $(g_V - \gamma_5 g_A)$

$$\mathcal{L}_{PV}^{NC} = -\frac{G_F}{\sqrt{2}} \Big[g_A^e (\bar{e}\gamma_\mu\gamma_5 e) \cdot \sum_q g_V^q (\bar{q}\gamma^\mu q) + g_V^e (\bar{e}\gamma_\mu e) \cdot \sum_q g_A^q (\bar{q}\gamma^\mu\gamma_5 q) \Big]$$

$$= -\frac{G_F}{2\sqrt{2}} \Big[\sum_q C_{1q} (\bar{e}\gamma_\mu\gamma_5 e) \cdot (\bar{q}\gamma^\mu q) + \sum_q C_{2q} (\bar{e}\gamma_\mu e) \cdot (\bar{q}\gamma^\mu\gamma_5 q) \Big]$$

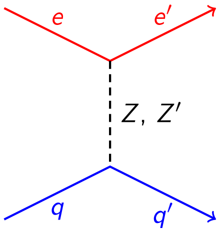

Electroweak Vector Charge of the Proton is Suppressed

Parity-violating electron scattering couplings

- Weak vector quark coupling: $C_{1q} = 2g_A^e g_V^q$ (γ^5 on e vertex)
- Weak axial quark coupling: $C_{2q} = 2g_V^e g_A^q$ (γ^5 on q vertex)

Particle	Electric charge	Weak vector charge ($\sin^2\theta_W \approx \frac{1}{4}$)
u	$+\frac{2}{3}$	$-2C_{1u} = +1 - \frac{8}{3}\sin^2\theta_W \approx +\frac{1}{3}$
d	$-\frac{1}{3}$	$-2C_{1d} = -1 + \frac{4}{3}\sin^2\theta_W \approx -\frac{2}{3}$
p(uud)	$+1$	$Q_W^p = 1 - 4\sin^2\theta_W \approx 0$
n(udd)	0	$Q_W^n = -1$

Proton's weak vector charge Q_W^p is approximately zero

Accidental suppression of the proton's weak charge in Standard Model makes it more sensitive to new physics!

Access to these weak vector charges by using parity-violation

We Use Spin to Access Weak Charges in Parity-Violation

Parity transformation: Inversion of spatial vectors $\vec{v} \to -\vec{v}$

- No change in the sign for angular momentum vectors ($\vec{S}$)

Tests using parity-violating electron scattering

- Polarized electrons (spin $\vec{S}$) on unpolarized target
- Instead of inverting $\vec{r} \to -\vec{r}$, $\vec{p} \to -\vec{p}$, but keeping $\vec{S} = \vec{S}$, we leave $\vec{r}$ and $\vec{p}$ unchanged but flip polarization or spin $\vec{S}$

Asymmetry A_{PV} between left and right scattering off nucleons

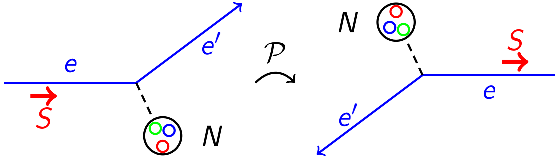

We Use Spin to Access Weak Charges in Parity-Violation

Parity transformation: Inversion of spatial vectors $\vec{v} \to -\vec{v}$

- No change in the sign for angular momentum vectors ($\vec{S}$)

Tests using parity-violating electron scattering

- Polarized electrons (spin $\vec{S}$) on unpolarized target
- Instead of inverting $\vec{r} \to -\vec{r}$, $\vec{p} \to -\vec{p}$, but keeping $\vec{S} = \vec{S}$, we leave $\vec{r}$ and $\vec{p}$ unchanged but flip polarization or spin $\vec{S}$

Asymmetry A_{PV} between left and right scattering off nucleons

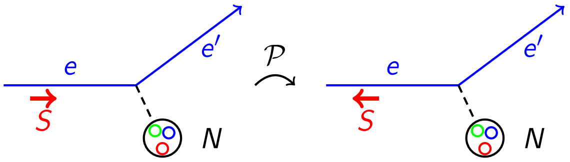

Difference in Cross Section is Encoded in Asymmetry.

Parity-violating asymmetry in electron scattering

- Difference between left- and right-handed scattering yield

$$A_{PV} = \frac{\sigma_R - \sigma_L}{\sigma_R + \sigma_L}$$

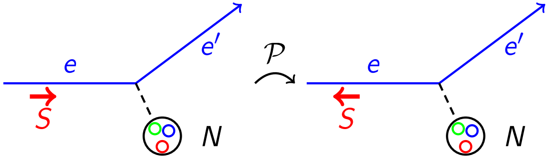

- Electromagnetic component is identical, hence subtracted out
- Parity-violating electroweak and new physics remains in A_{PV}

Parity-Violating Asymmetry Reduces to the Weak Charge

Asymmetry between left and right helicity

$$A_{PV} = \frac{\sigma_L - \sigma_R}{\sigma_L + \sigma_R} \quad \text{with} \quad \sigma = \left| \; \cdots \; \right|^2$$

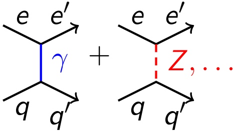

Interference of photon and weak boson exchange

$$\mathcal{M}^{EM} \propto \frac{1}{Q^2} \qquad \mathcal{M}^{NC}_{PV} \propto \frac{1}{M_Z^2 + Q^2}$$

$$A_{PV} = \frac{\sigma_R - \sigma_L}{\sigma_R + \sigma_L} \propto \frac{\mathcal{M}^{NC}_{PV}}{\mathcal{M}^{EM}} \propto \frac{Q^2}{M_Z^2} \quad \text{when } Q^2 \ll M_Z^2$$

Parity-Violating Asymmetry Reduces to the Weak Charge

Asymmetry between left and right helicity

$$A_{PV} = \frac{\sigma_L - \sigma_R}{\sigma_L + \sigma_R} \quad \text{with} \quad \sigma = \left| \; \cdots \; \right|^2$$

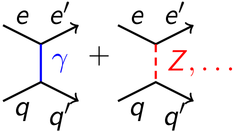

Interference of photon and weak boson exchange for protons

$$A_{PV}(p) = \frac{-G_F Q^2}{4\pi\alpha\sqrt{2}} \left[\frac{\epsilon G_E G_E^Z + \tau G_M G_M^Z - (1 - 4\sin^2\theta_W)\epsilon' G_M G_A^Z}{\epsilon (G_E)^2 + \tau (G_M)^2} \right]$$

In the forward elastic limit $Q^2 \to 0$, $\theta \to 0$ (plane wave)

$$A_{PV}(p) \xrightarrow{Q^2 \to 0} \frac{-G_F Q^2}{4\pi\alpha\sqrt{2}} \left[Q_W^p + Q^2 \cdot B(Q^2) \right] \approx -230\,\text{ppb} \propto Q_W^p$$

Parity-Violating Asymmetry Reduces to the Weak Charge

Asymmetry between left and right helicity

$$A_{PV} = \frac{\sigma_L - \sigma_R}{\sigma_L + \sigma_R} \quad \text{with} \quad \sigma = \left| \; \cdots \; \right|^2$$

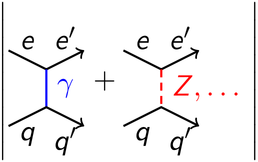

Interference of photon and weak boson exchange for electrons

$$A_{PV}(e) = mE \frac{G_F}{\pi\alpha\sqrt{2}} \left[\frac{4\sin^2\theta}{(3+\cos^2\theta)^2} \right] Q_W^e$$

Direct connection from asymmetry to weak charge of electron

$$A_{PV}(e) \approx 35\,\text{ppb} \propto Q_W^e$$

No hadronic uncertainty due to $B(Q^2)$ form factor term

Strategy to Measure Parts-Per-Billion: All The Events!

Event versus integration mode

- Event mode (the good ol' nuclear/particle way)
  - each event individually registered
  - event selection or rejection possible

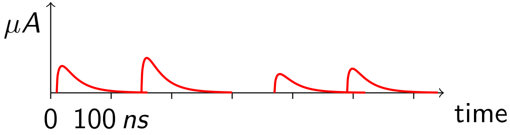

- Integrating mode (current mode)
  - high event rates possible (event every nanosecond!)
  - no suppression of background events possible

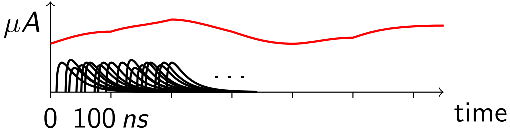

We Measure Time-Dependent Integrated Detector Signal

Current mode with 1 kHz helicity reversals

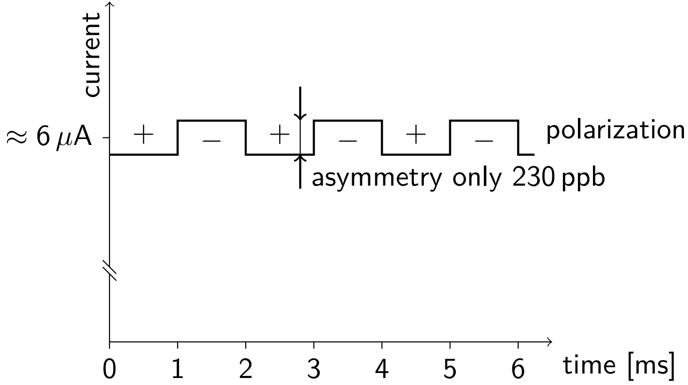

- Collect many polarization windows: 2 year long experiment
- Counting mode at 1 MHz would have taken 7000 years. . .

We Measure Time-Dependent Integrated Detector Signal

Current mode with 1 kHz helicity reversals

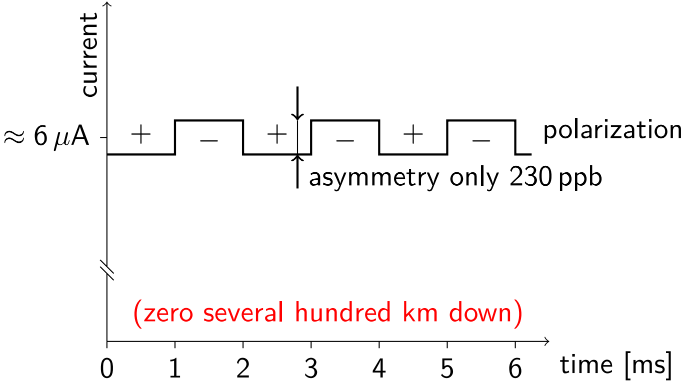

- Collect many polarization windows: 2 year long experiment
- Counting mode at 1 MHz would have taken 7000 years...

We Measure Time-Dependent Integrated Detector Signal

Current mode with 1 kHz helicity reversals

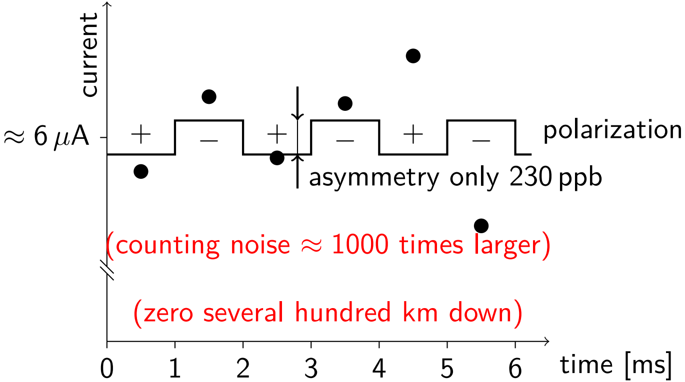

- Collect many polarization windows: 2 year long experiment
- Counting mode at 1 MHz would have taken 7000 years. . .

Section 2

Parity-Violating Electroweak Experiments at Jefferson Lab

Parity-Violating Electroweak Experiments at Jefferson Lab

Q_{Weak} Experiment

- Measurement of Q_W^p in $\vec{e}p \to e'p$ on protons in hydrogen
- Completed, preliminary results, full results in Fall 2017
- Ongoing analysis effort, constitutes the bulk of this talk

MOLLER Experiment

- Measurement of Q_W^e in $\vec{e}e \to e'e$ on electrons in hydrogen
- Planned for running at Jefferson Lab 12 GeV

PV-DIS and SoLID Experiments

- Measurement of $C_{1,2q}$ in $\vec{e}p \to e'p$ on hydrogen, deuterium
- Completed at 6 GeV, planned at Jefferson Lab 12 GeV

Where is Jefferson Lab?

Newport News, Virginia

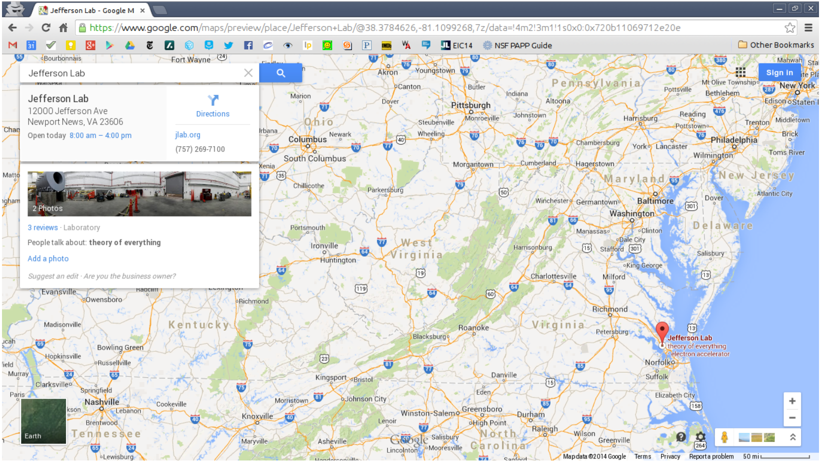

What is Jefferson Lab?

Jefferson Lab Overview

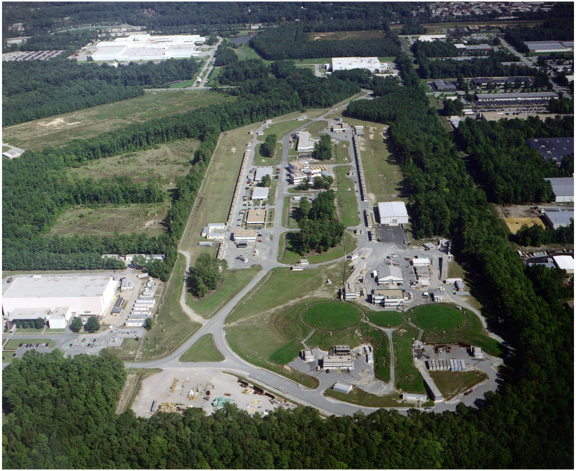

Section 3

The Q_{Weak} Experiment

The Q_{Weak} Experiment: Overview

- Precision measurement of a quantity suppressed by fundamental symmetries ($Q_W^p \approx 0$, asymmetry of 230 ppb)
- Elastic scattering of electron beam on proton target to measure the proton weak charge Q_W^p to a precision of 4%

Pushing the envelope of intensity (more events)

- Higher beam current (150 μA versus usually $< 100\,\mu$A)
- Longer cryo-target (35 cm versus 20 cm)
- Higher event rates up to 800 MHz (integration)

Pushing the envelope of precision (better measurements)

- Electron beam polarization precision of 1% at 1 GeV
- Helicity-correlated asymmetries at ppb level

The Q_{Weak} Experiment: Overview

Collimator-Magnet-Collimator focusing spectrometer

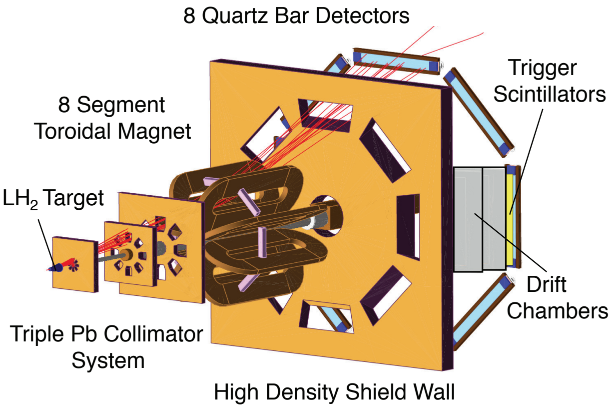

"The Qweak Experimental Apparatus," NIM A 781, 105 (2015); `http://dx.doi.org/10.1016/j.nima.2015.01.023`

The Q_{Weak} Experiment: Overview

Collimator-Magnet-Collimator focusing spectrometer

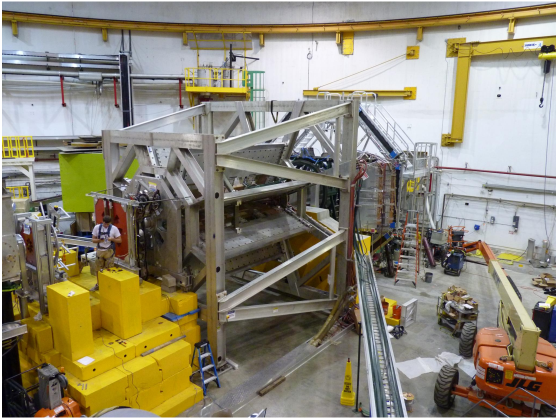

"The Qweak Experimental Apparatus," NIM A 781, 105 (2015);
`http://dx.doi.org/10.1016/j.nima.2015.01.023`

The Q_{Weak} Experiment: High Power Cryotarget

Operational Parameters

- Transverse flow: 2.8 m/s
- Target length: 35 cm
- Beam current: 150 μA
- Heating power: 2.5 kW

Power for other cryotargets

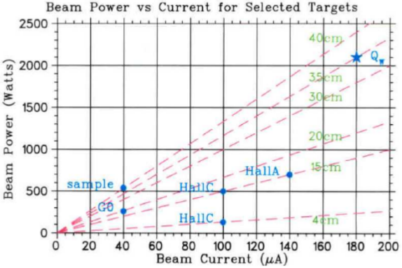

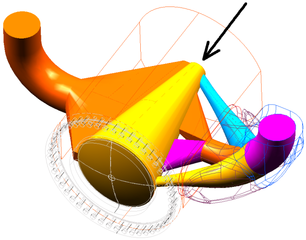

Design with CFD

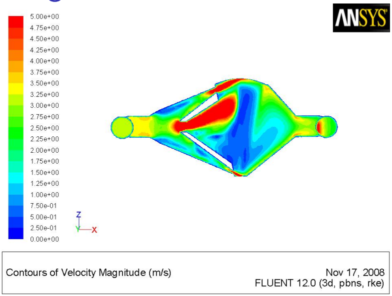

The Q_{Weak} Experiment: High Power Cryotarget

Low-frequency 'boiling' noise

- Helicity flip rate 960 Hz → 240 Hz (quartet cycles)
- Target density fluctuations at low frequencies occur
- Power spectrum of signal

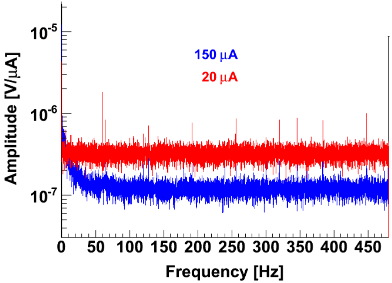

Current dependence

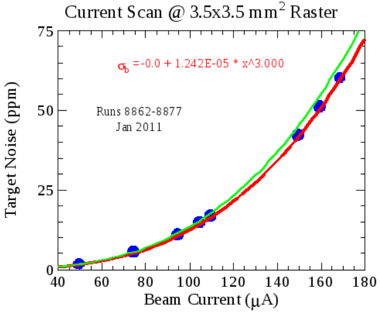

- Additional noise smaller than statistical width
- Consistent for different current and beam rasters
- Current to 180 μA

The Q_{Weak} Experiment: Main Detector

Preradiated Čerenkov detector bars

- 8 fused silica radiators, 2 m long × 18 cm × 1.25 cm
- Pb preradiator tiles to reduce low-energy tracks (neutrals)
- Light collection: total internal reflection
- 5 inch PMTs with gain of 2000, low dark current
- 800 MHz electron rate per bar, defines counting noise

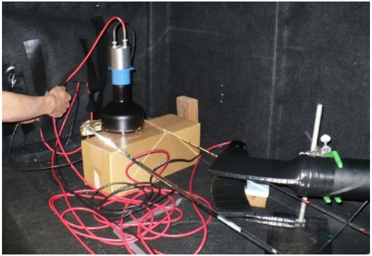

The Q_{Weak} Experiment: Kinematics in Event Mode

Reasons for a tracking system?

- Determine Q^2, note: $A_{meas} \propto Q^2 \cdot \left(Q_W^p + Q^2 \cdot B(Q^2)\right)$
- Main detector light output and Q^2 position dependence
- Contributions from inelastic background events

Instrumentation of only two octants

- Horizontal drift chambers for front region (Va Tech)
- Vertical drift chambers for back region (W&M)
- Rotation allows measurements in all eight octants

Track reconstruction

- Straight tracks reconstructed in front and back regions
- Front and back partial tracks bridged through mag field

The Q_{Weak} Experiment: Improved Beam Polarimetry

Requirements on beam polarimetry

- Largest experimental uncertainty in Q_{Weak} experiment
- Systematic uncertainty of 1% (on absolute measurements)

Upgrade existing Møller polarimeter ($\vec{e} + \vec{e} \rightarrow e + e$)

- Scattering off atomic electrons in magnetized iron foil
- Limited to separate, low current runs ($I \approx 1\,\mu$A)

Construction new Compton polarimeter ($\vec{e} + \vec{\gamma} \rightarrow e + \gamma$)

- Compton scattering of electrons on polarized laser beam
- Continuous, non-destructive, high precision measurements

The Q_{Weak} Experiment: Improved Beam Polarimetry

Compton polarimeter

- Beam: 150 μA at 1.165 GeV
- Chicane: interaction region 57 cm below straight beam line
- Laser system: 532 nm green laser
  - 10 W CW laser with low-gain cavity
- Photons: $PbWO_4$ scintillator in integrating mode
- Electrons: Diamond strips with 200 μm pitch

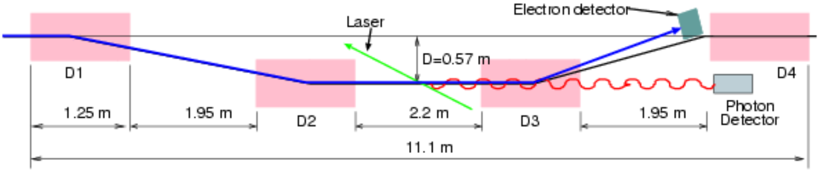

The Q_{Weak} Experiment: Beam Polarimetry

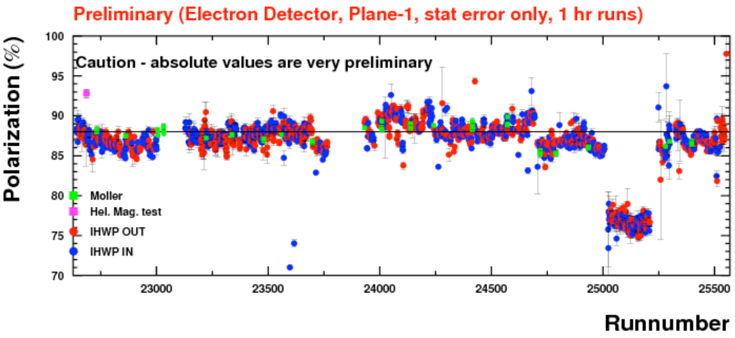

Møller polarimetry

- New beamline, refurbished
- Invasive measurements
- Polarization larger than anticipated: 86% to 88%

Compton polarimetry

- Excellent performance
- Continuous measurements
- Operates at full 180 μA
- Great statistical precision

Data Quality: Slow Helicity Reversal

$\lambda/2$-plate and Wien filter changes

- Insertable $\lambda/2$-plate (IHWP) in injector allows ‘analog’ flipping helicity frequently
- Wien filter: another way of flipping helicity (several weeks)
- Each ‘slug’ of 8 hours consists of same helicity conditions

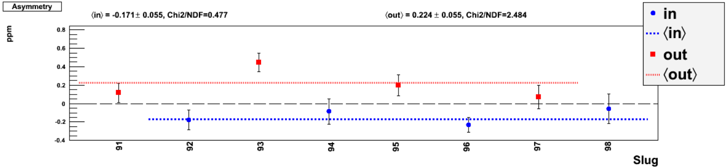

- Preliminary asymmetries: 60 ppb blinded, not corrected, not regressed! And only 8 of hundreds of slugs. . .
- Average asymmetries are consistent with sign change

Weak Charge in Preliminary Agreement with Prediction

First results based on subset of the data in 2013

- Publication in Phys. Rev. Lett. 111, 141803 (2013)
- Based on only 4% of the total data set: first experiment with direct access to proton's weak charge
- 25 times more data available: projected release in Fall 2017

Global analysis method by Young, Roche, Carlini, Thomas

- Fit of parity-violating asymmetry data on H, D, ^{4}He, up to $Q^2 = 0.63\,\mathrm{GeV}^2$, and rotated to zero forward angle
- Free parameters were C_{1u}, C_{1d}, strange charge radius ρ_s and magnetic moment μ_s, and isoscalar axial form factor (zero at tree level)
  - $Q_W^p(\mathrm{PVES}) = 0.064 \pm 0.012$ (our result with world data)
  - $Q_W^p(\mathrm{SM}) = 0.0710 \pm 0.0007$ (theoretical expectation)

First Determination of the Weak Charge of the Proton

Intercept of reduced asymmetry at $Q^2 = 0$

$$\overline{A_{PV}} = \frac{A_{PV}}{A_0} = Q_W^p + Q^2 \cdot B(Q^2, \theta = 0) \quad \text{with} \quad A_0 = -\frac{G_F Q^2}{4\pi\alpha\sqrt{2}}$$

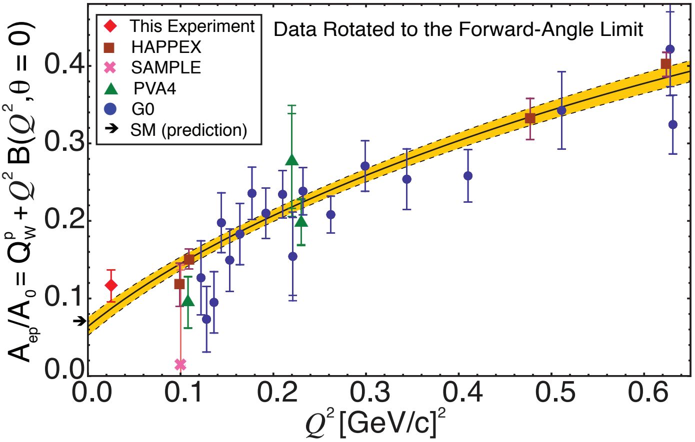

Determination of the Weak Charge of the Proton

Extraction from just parity-violating electron scattering, including the new Q_{Weak} results

$$Q_W^p(\mathrm{PVES}) = 0.064 \pm 0.012$$

In agreement with prediction in the Standard Model

$$Q_W^p(\mathrm{SM}) = 0.0710 \pm 0.0007$$

Determination of the Weak Vector Charges of the Quarks

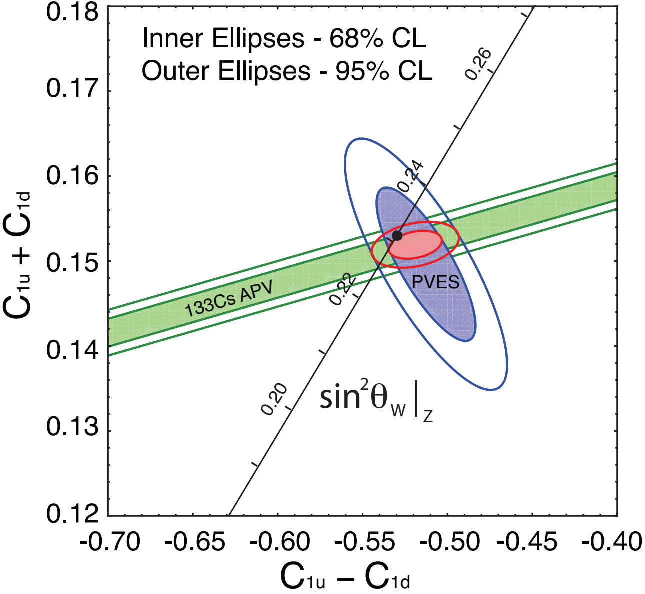

Determination of the Electroweak Mixing Angle

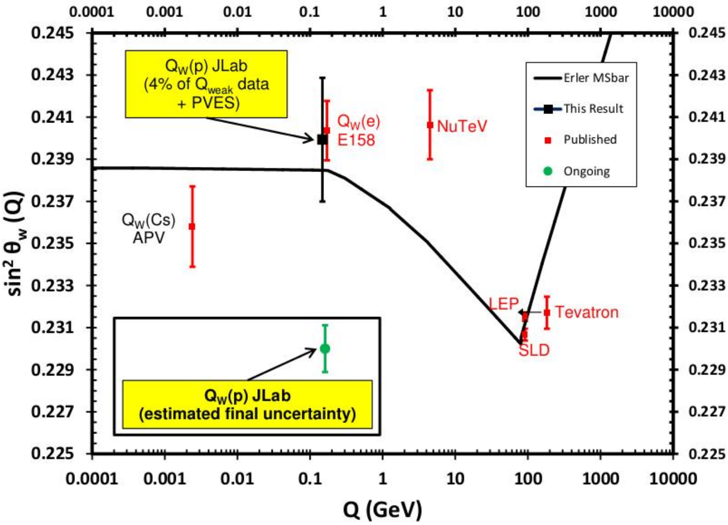

Determination of the Weak Vector Charges of the Quarks

Global fit of all atomic and electron scattering data

- Determination of weak charge of the proton
  - $Q_W^p(\text{PVES+APV}) = 0.063 \pm 0.012$
  - $Q_W^p(\text{SM}) = 0.0710 \pm 0.0007$
- Extraction of weak vector quark couplings possible
  - $C_{1u} = -0.1835 \pm 0.0054$
  - $C_{1d} = 0.3355 \pm 0.0050$
- Determination of weak charge of the neutron
  - $Q_W^n(\text{PVES+APV}) = -0.975 \pm 0.010$
  - $Q_W^n(\text{SM}) = -0.9890 \pm 0.0007$

Largest Uncertainties in Preliminary Q_{Weak} Result?

All uncertainties in **ppb**	ΔA_{corr}		$\delta(A_{PV})$
Beam polarization P	-21		5
Kinematics R_{total}	5		9
Dilution $1/(1-\sum f_i)$	-7		
Beam asymmetry	-40		13
Transverse pol. A_T	0		5
Detector non-linearity	0		4
Backgrounds:		$\delta(f_i)$	$\delta(A_i)$
Aluminum (b_1)	-58	4	8
Beamline (b_2)	11	3	23
Neutrals (b_3)	0	1	1
Inelastic (b_4)	1	1	1

$$A_{PV} = R_{total} \frac{\frac{A_{msr}}{P} - \sum f_i A_i}{1 - \sum f_i}$$

Largest Uncertainties in Preliminary Q_{Weak} Result?

All uncertainties in **ppb**	ΔA_{corr}		$\delta(A_{PV})$
Beam polarization P	-21		5
Kinematics R_{total}	5		9
Dilution $1/(1-\sum f_i)$	-7		
Beam asymmetry	-40		13
Transverse pol. A_T	0		5
Detector non-linearity	0		4
Backgrounds:		$\delta(f_i)$	$\delta(A_i)$
Aluminum (b_1)	-58	4	8
Beamline (b_2)	11	3	23
Neutrals (b_3)	0	1	1
Inelastic (b_4)	1	1	1

$$A_{PV} = R_{total} \frac{\frac{A_{msr}}{P} - \sum f_i A_i}{1 - \sum f_i}$$

Helicity-Correlated Beam Properties Are Understood

Measured asymmetry depends on beam position, angle, energy

- Well-known and expected effect for PVES experiments
- "Driven" beam to check sensitivities from "natural" jitter

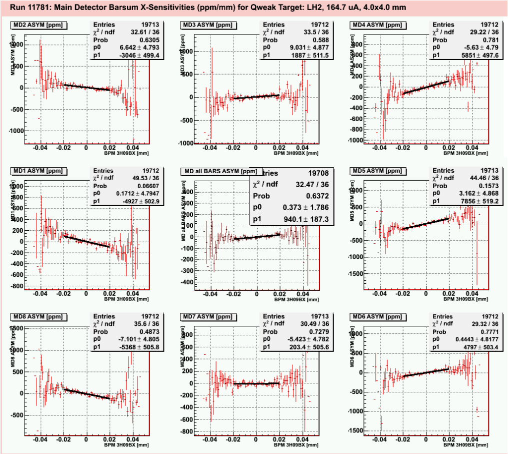

Helicity-Correlated Beam Properties Are Understood

Sensitivities are used to correct measured asymmetry

- $A_{corr} = \sum_i \frac{\partial A}{\partial x_i} \Delta x_i$ with beam parameters $i = x, y, x', y', E$
- Sensitivities (derivatives) from simultaneous regression fits

Excellent agreement between natural and driven beam motion

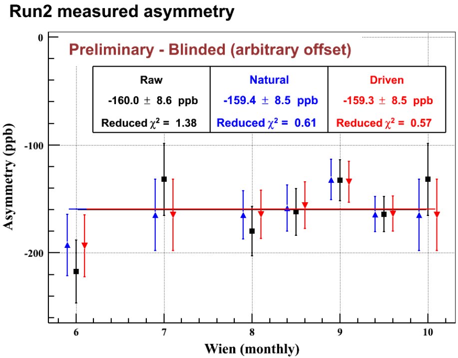

- Figure includes about 50% of total dataset for Q_{Weak} experiment
- No other corrections applied to this data

However, Some Beamline Background Correlations Remain

After regression, correlation with background detectors

- Luminosity monitors & spare detector in super-elastic region
- Background asymmetries of up to 20 ppm (that's huge!)

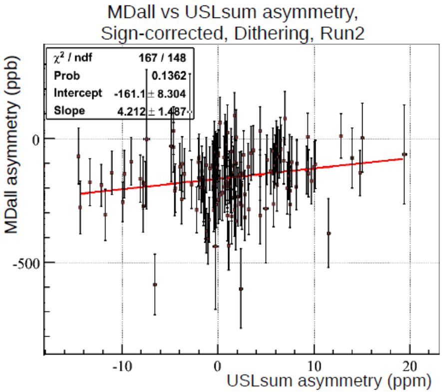

Figure 6.19: The correlation between MDall and USLsum asymmetries in the Sign-corrected formulation, averaged at the slug scale over the Run2 Modulation dataset. The extracted correlation slope is the correction factor $C^{\mathrm{BB}}_{\mathrm{MD\text{-}USL}}$ for the BB correction (6.6).

However, Some Beamline Background Correlations Remain

Hard work by grad students: now understood, under control

- Partially cancels with slow helicity reversal (half-wave plate)
- Likely caused by large asymmetry in small beam halo or tails
- Scattering off the beamline and/or “tungsten plug”

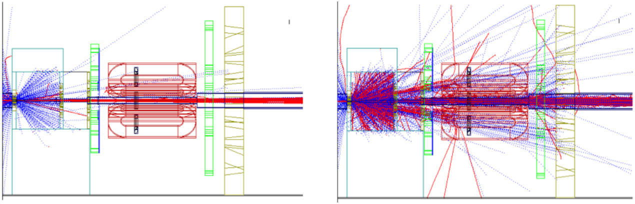

Qualitatively new background for PVES experiments at JLab

- Second regression using asymmetry in background detectors
- Measurements with blocked octants to determine dilution factor ($f_{b_2}^{MD} = 0.19\%$)

Beamline Background Corrections Are Under Control

Beamline background correction improve statistical consistency

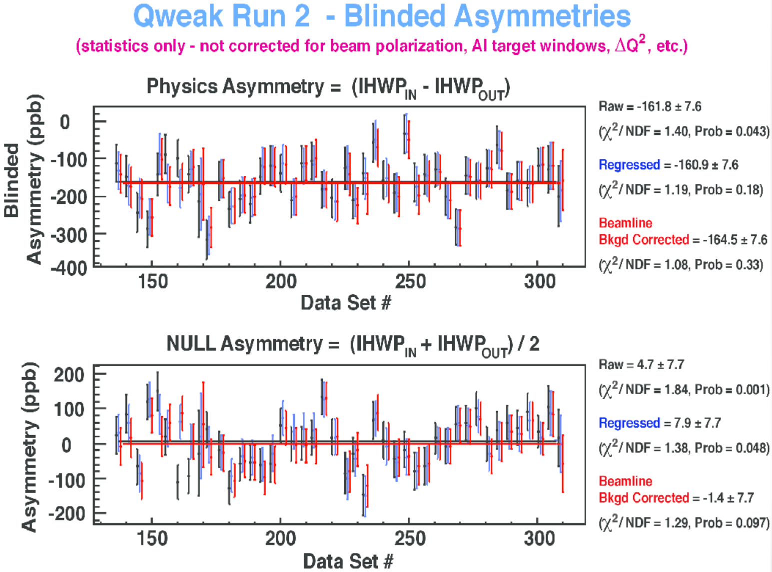

Sensitivity to New Physics

New parity-violating physics

- Consider effective contact interaction
- Coupling constant g, mass scale Λ
- Effective charges $h_V^u = \cos\theta_h$ and $h_V^d = \sin\theta_h$

Effective Lagrangian (Erler *et al.*, PRD 68, 016006 (2003))

$$\begin{aligned}\mathcal{L}_{e-q}^{PV} &= \mathcal{L}_{SM}^{PV} + \mathcal{L}_{New}^{PV} \\ &= -\frac{G_F}{\sqrt{2}}\bar{e}\gamma_\mu\gamma_5 e \sum_q C_{1q}\bar{q}\gamma^\mu q + \frac{g^2}{4\Lambda^2}\bar{e}\gamma_\mu\gamma_5 e \sum_q h_q^V \bar{q}\gamma^\mu q\end{aligned}$$

Sensitivity to New Physics

Determination of weak charge of the proton

- Assume agreement with Standard Model within ΔQ_W^p
- What are the limits on $\frac{\Lambda}{g}$?

Limits on new physics energy scale

$$\frac{\Lambda}{g} = \frac{1}{2}\left(\sqrt{2}G_F\Delta Q_W^p\right)^{-1/2}$$

- Limits from $\Delta Q_W^p = 0.005$: $\frac{\Lambda}{g} > 1.7\,\text{TeV}$ at $1\,\sigma$
- For comparison with LHC results: $g^2 = 4\pi$
- Lower limit $\Lambda > 5.4\,\text{TeV}$ at 95% C.L.

Progress on Q_{Weak} Data Analysis

A lot of progress has been made already

- Completed data-taking in May 2012
- Published first determination of proton's weak charge and global analysis in PRL in October 2013
  - $Q_W^p(PVES + APV) = 0.063 \pm 0.012$ with only 4% of the data

Unprecedented precision come with inevitable surprises

- Blind analysis precludes "incremental" preliminary results
- Discovered qualitatively new "beamline background" noise
- Discovered another qualitatively new systematic (non-noise) background

Progress on Q_{Weak} Data Analysis

A lot of progress has been made already

- Discovered another qualitatively new systematic (non-noise) background
  - Various microscopic explanations consistent with effect
  - Geant4 simulations & detector post-mortems on-going
  - Confident that we can understand this effect better

The Q_{Weak} Experiment: Timeline

- Double-scattering effect studies were our last hangup
- Unblinding: March 31, 2017
- Publication and release during the summer/fall (DNP meeting)
- Stay tuned!

The Q_{Weak} Experiment: Projections

Reduced parity-violating asymmetry

- This was all with only 4% of total data!
- Projected result with full data set (25 times more data)

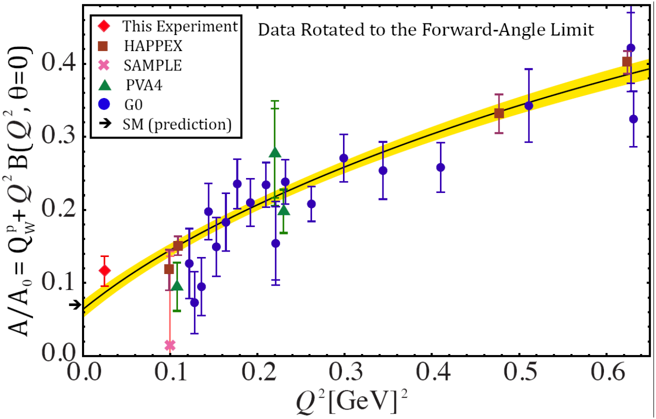

The Q_{Weak} Experiment: Projections

Reduced parity-violating asymmetry

- This was all with only 4% of total data!
- Projected result with full data set (25 times more data)

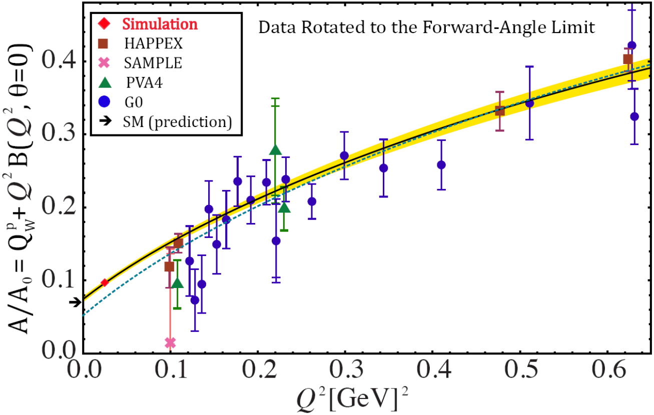

The Q_{Weak} Experiment: Ancillary Measurements

Upcoming ancillary results

- Aluminum parity-violating asymmetry
- Elastic transverse asymmetry (two-photon exchange effects)
- Nuclear-elastic transverse asymmetry (Coulomb interaction)
- $N \to \Delta$ asymmetry at two beam energies
- Transverse asymmetry in Δ production
- Non-resonant inelastic parity-violating asymmetry (γZ box diagram)
- Non-resonant inelastic transverse asymmetry
- Pion photoproduction parity-violating asymmetries
- Pion photoproduction transverse asymmetries

Section 4

The MOLLER Experiment

The MOLLER Experiment

Measurement of the electroweak mixing angle at low energy

- Elastic scattering of electrons on electrons in hydrogen
- Precision measurement of the weak charge of the electron $Q_W^e \approx 0$ at 11 GeV
  - Asymmetry $A_{PV} \approx 35.6\,\text{ppb}$, with precision $\delta A_{PV} = \pm 0.7\,\text{ppb}$
  - Precision $\delta Q_W^e \approx \pm 2.1\%$, $\delta \sin^2 \theta_W = \pm 0.1\%$

Pushing the envelope of intensity (more events)

- Even higher luminosity: 85 μA on 1.5 m long cryo-target
- Event rates up to 150 GHz (integrated, of course)

Pushing the envelope of precision

- Electron beam polarization precision of 0.4% at 11 GeV

The MOLLER Experiment

Experimental Layout

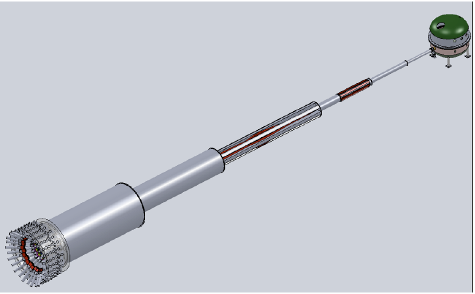

- Long, narrow hybrid toroidal spectrometer system to select very forward events
- Focusing of *ee* and *ep* on segmented quartz detector rings

The MOLLER Experiment

Experimental Layout

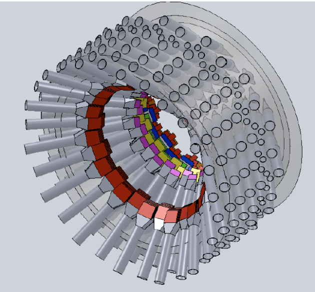

- Long, narrow hybrid toroidal spectrometer system to select very forward events
- Focusing of *ee* and *ep* on segmented quartz detector rings

Section 5

PV-DIS and SoLID Experiments

PV-DIS and SoLID Experiments

Analogy with Deep Inelastic Scattering

$$\frac{d^2\sigma}{d\Omega dE'} = \frac{\alpha^2}{4E^2 \sin^4 \frac{\theta}{2}} \left(\frac{2}{M} F_1(x) \sin^2 \frac{\theta}{2} + \frac{1}{\nu} F_2(x) \cos^2 \frac{\theta}{2} \right)$$

Quark structure through **DIS**

- $F_2(x) = x \sum_q e_q^2 (q + \bar{q}) \approx 2x F_1(x)$ (Callan-Gross)

Quark structure through **PV-DIS**: interference of γZ

- $F_2^{\gamma Z}(x) = x \sum_q e_q g_q^V (q + \bar{q}) \to a_1(x) \sim \sum_q e_q C_{1q} (q + \bar{q})$
- $F_3^{\gamma Z}(x) = x \sum_q e_q g_q^A (q - \bar{q}) \to a_3(x) \sim \sum_q e_q C_{2q} (q - \bar{q})$

PV-DIS and SoLID Experiments

Recent Results from PV-DIS at 6 GeV

- Published in Nature 506, p67 (February 2014)
- First evidence at 95% C.L. that the weak axial quark couplings C_{2q} are non-zero (as predicted by the Standard Model)
- Exclusion limits for contact interactions $\Lambda^- > 4.8\,\text{TeV}$ and $\Lambda^+ > 5.8\,\text{TeV}$

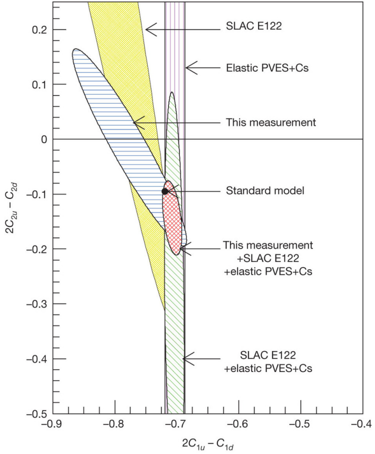

PV-DIS and SoLID Experiments

Solenoidal Large Intensity Device

- $2\,\text{GeV} < p < 8\,\text{GeV}$
- $2\,\text{GeV}^2 < Q^2 < 10\,\text{GeV}^2$
- $0.2 < x < 1$
- 40% azimuthal acceptance
- $\mathcal{L} \approx 5 \cdot 10^{35}\,\text{s}^{-1}\text{cm}^{-2}$

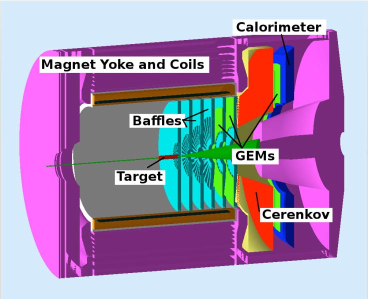

Experimental design

- Counting mode at rate $> 200\,\text{kHz}$, 30 independent sectors
- Baffles filter low energy and neutral particles (no line of sight)
- Light gas Čerenkov for 1000–200 : 1 rejection of low-E π^-
- Electromagnetic calorimeter for 50 : 1 π^- rejection

PV-DIS and SoLID Experiments: Weak Axial Couplings

Projected Precision on C_{1q} and C_{2q} Couplings

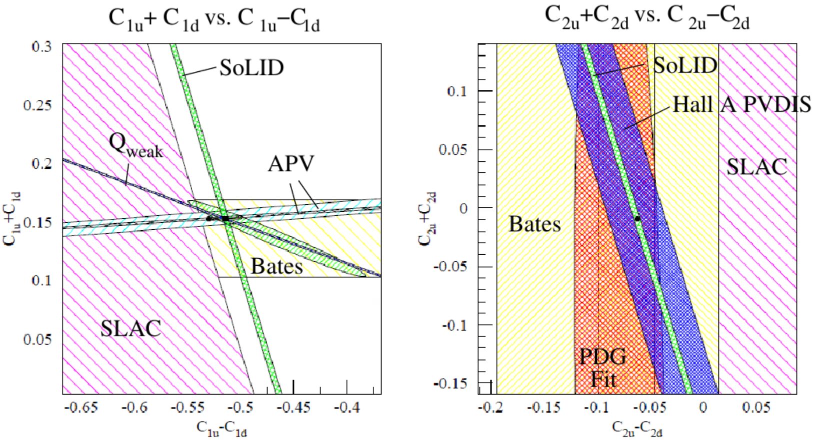

Section 6

Summary

Summary

The Q_{Weak} experiment

- Elastic $\vec{e}$-p scattering on liquid hydrogen target
- Precision measurement of a proton weak charge $Q_W^p \approx 0$, quantity suppressed by fundamental symmetries
- First determination of the weak charge of the proton
  - With only 4% of the full data set
  - $Q_W^p(PVES + APV) = 0.063 \pm 0.012$
  - Weak charge is in agreement with Standard Model
- Results from full data set anticipated in fall 2014

Broad program of electroweak precision measurements

- PV-DIS: weak axial quark couplings are non-zero at 95% C.L.
- MOLLER, SoLID: precision measurements of mixing angle and weak quark couplings

Additional Material

Section 7

Parity-Violating and Parity-Conserving Nuclear Asymmetries

Ancillary Measurements: Aluminum Target Walls

Aluminum asymmetry (preliminary)

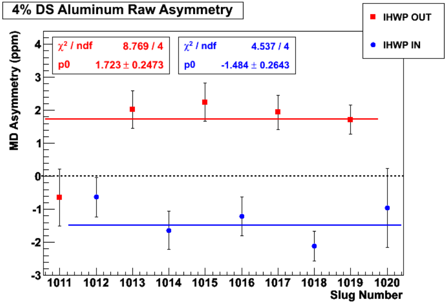

- Asymmetry consistent with order of magnitude expected

- Asymmetry: few ppm
- Dilution f of 3%
- Correction ≈ 20%

Dilution measurement (preliminary)

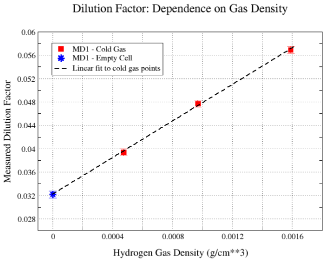

Ancillary Measurements: Inelastic Transitions

$N \to \Delta$ asymmetry (projected)

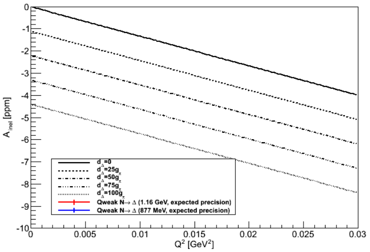

- In analysis, no result yet
- Expected precision 1 ppm
- $Q^2 = 0.025\,\text{GeV}^2$

- Asymmetry: few ppm
- Dilution f of 0.1%
- Correction $\approx$ 1%

Simulation benchmark (preliminary)

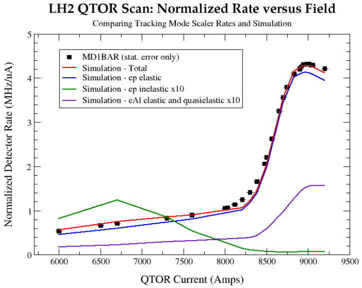

Ancillary Measurements: Inelastic Transitions

$N \to \Delta$ asymmetry (projected)

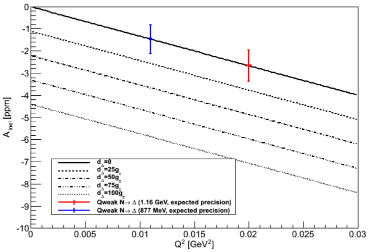

- In analysis, no result yet
- Expected precision 1 ppm
- $Q^2 = 0.025\,\mathrm{GeV}^2$

- Asymmetry: few ppm
- Dilution f of 0.1%
- Correction $\approx$ 1%

Simulation benchmark (preliminary)

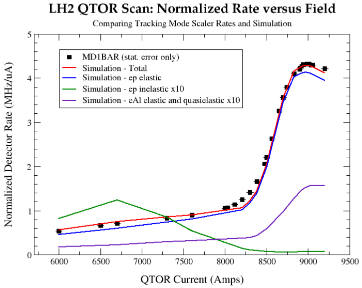

Ancillary Measurements: Transverse Asymmetry

- In main measurement, not 100% longitudinal polarization
- Transversely polarized beam (H or V) on unpolarized target
- Parity-conserving, T-odd transverse asymmetry of order ppm

$$B_n = \frac{2\Im(T_{1\gamma}^* \cdot T_{2\gamma})}{|T_{1\gamma}|^2}$$

- Access to imaginary part of 2-photon exchange amplitude $T_{2\gamma}$
- Extensive transverse spin program:
  - elastic $\vec{e}p$ in H, C, Al at $E = 1.165\,\mathrm{GeV}$
  - inelastic $\vec{e}p \to \Delta$ in H, C, Al at $E = 0.877\,\mathrm{GeV}$ and $1.165\,\mathrm{GeV}$
  - elastic $\vec{e}e$ in H at $E = 0.877\,\mathrm{GeV}$
  - deep inelastic $\vec{e}p$ in H at $W = 2.5\,\mathrm{GeV}$
  - pion electro-production in H at $E = 3.3\,\mathrm{GeV}$

Ancillary Measurements: Transverse Asymmetry on H

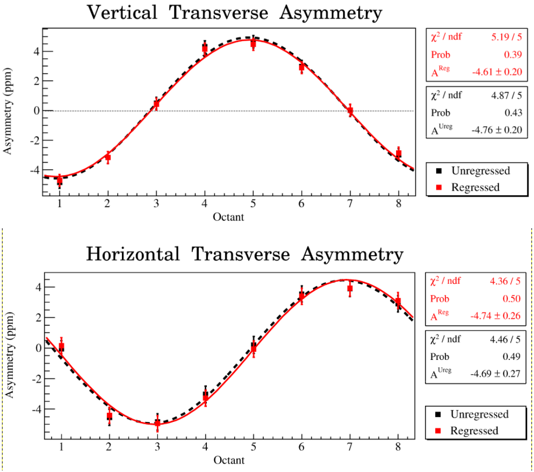

- Vertical and horizontal polarization: 90° phase shift
- Observe the expected cancellation with slow helicity reversal

Ancillary Measurements: Transverse Asymmetry on H

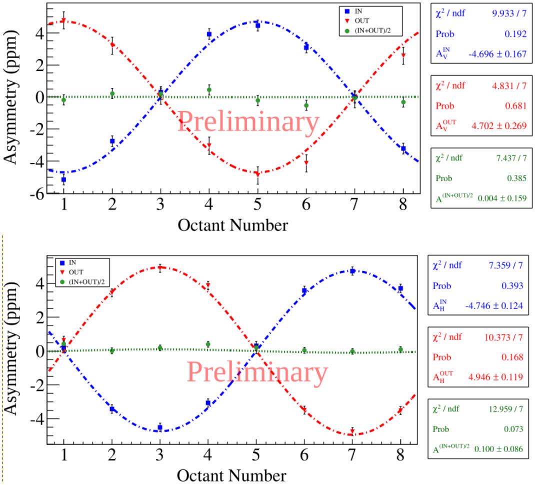

- Vertical and horizontal polarization: 90° phase shift
- Observe the expected cancellation with slow helicity reversal

Ancillary Measurements: Transverse Asymmetry on H

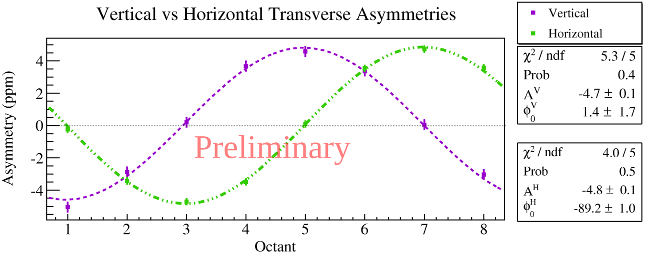

- Shown asymmetries not corrected for backgrounds or polarization
- Preliminary transverse asymmetry in $\vec{e}p$ in hydrogen: $B_n = -5.35 \pm 0.07(\text{stat}) \pm 0.15(\text{syst})\,\text{ppm}$
- More precise than any other measurement by a factor 5
- Theory: Pasquini & Vanderhaeghen, Afanasev & Merenkov, Gorchtein

Ancillary Measurements: Transverse Asymmetry on H

Theoretical interpretation

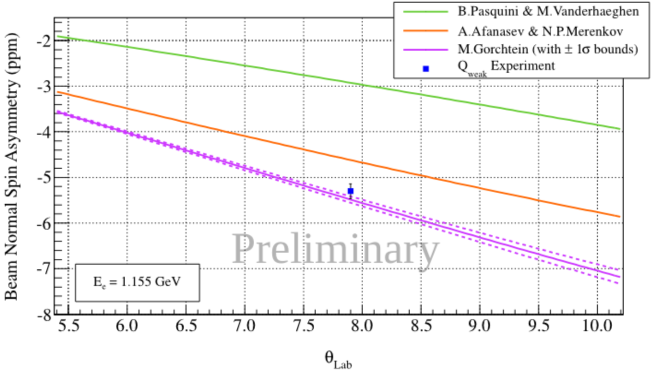

- Theory: Pasquini & Vanderhaeghen, Afanasev & Merenkov, Gorchtein

Ancillary Measurements: Transverse Asymmetry on C, Al

Aluminum: non-zero transverse asymmetry (uncorrected data)

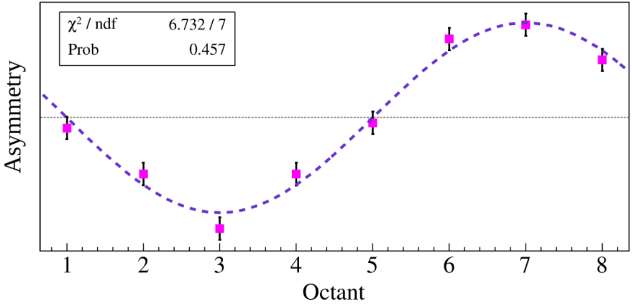

- Aluminum target was alloy with 10% contamination
- Needs corrections for quasielastic and inelastic scattering, and for nuclear excited states(?)

Ancillary Measurements: Transverse Asymmetry on C, Al

Projected uncertainties for C and Al transverse asymmetries

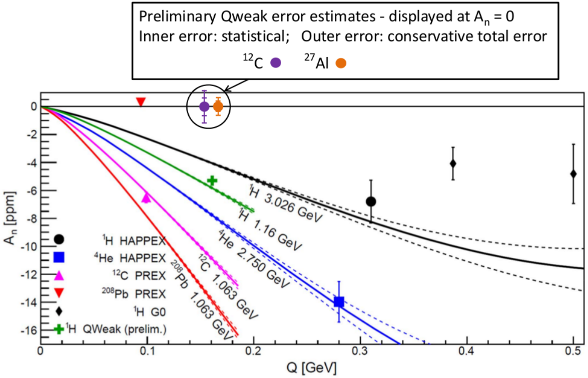

- Theory from Phys. Rev. C77, 044606 (2008)
- Pb data from PRL 109, 192501 (2012)

Data Quality: Understanding the Width

Asymmetry width

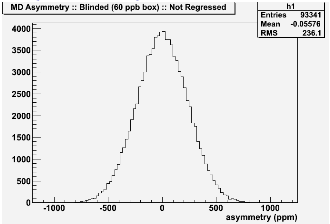

Battery width

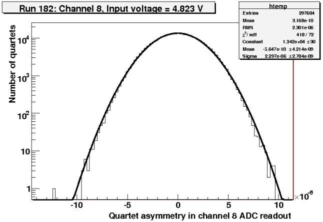

Measurement

- 240 Hz helicity quartets ($+--+$ or $-++-$)
- Uncertainty $= RMS/\sqrt{N}$
- 200 ppm in 4 milliseconds
- < 1 ppm in 5 minutes

Asymmetry width

- Pure counting statistics ≈ 200 ppm
- $+$ detector resolution ≈ 90 ppm
- $+$ current monitor ≈ 50 ppm
- $+$ target boiling ≈ 57 ppm
- $=$ observed width ≈ 233 ppm

Data Quality: Helicity-Correlated Beam Properties

Natural beam motion

- Measured asymmetry correlated with beam position and angles
- False asymmetries
- Linear regression removes effect:
  $A_c = \sum_i \frac{\partial A}{\partial x_i} \Delta x_i$
  $i = x, y, x', y', E$

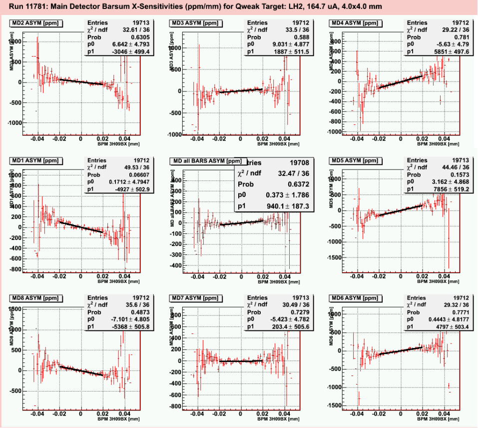

Data Quality: Helicity-Correlated Beam Properties

Driven beam motion

- Deliberate motion
- $i = x, y, x', y', E$

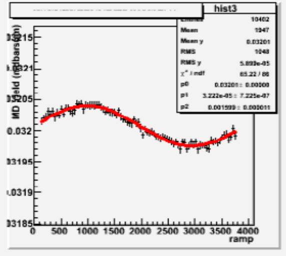

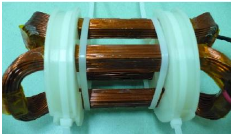

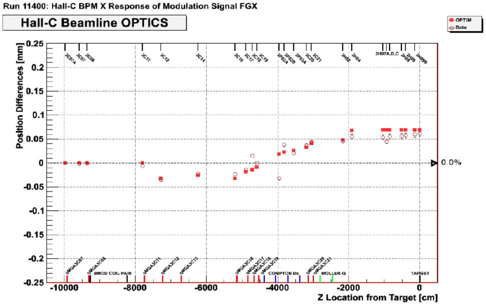

- Sensitivity slopes $\frac{\partial A}{\partial x_i}$ determined from natural beam motion or from beam modulation $\rightarrow$ results consistent between methods
- Actual regression corrections smaller than specifications

Section 8

First Results from the Q_{Weak} Experiment

Ancillary Measurements: Transverse Asymmetry

- Transversely polarized beam on unpolarized target
- Parity-conserving (T-odd) transverse asymmetry of order ppm

$$B_n = \frac{2\Im(T_{1\gamma}^* \cdot T_{2\gamma})}{|T_{1\gamma}|^2}$$

- Access to imaginary part of 2-photon exchange amplitude $T_{2\gamma}$
- False asymmetry for parity-violating asymmetry A_{PV} due to residual transverse polarization and broken azimuthal symmetry

Ancillary Measurements: Transverse Asymmetry

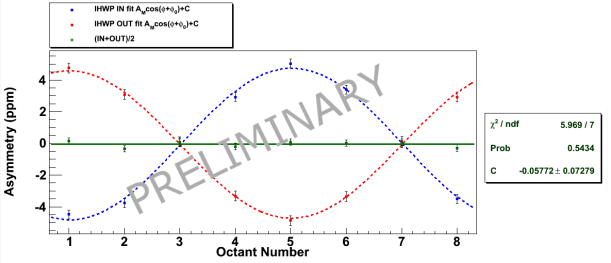

- Vertical polarization: cancellation with helicity reversal
- Horizontal polarization: 90° phase shift from vertical
- Shown asymmetries not corrected for backgrounds or polarization
- Preliminary transverse asymmetry: $B_n = -5.27 \pm 0.07(\text{stat}) \pm 0.14(\text{syst})\,\text{ppm}$
- Transverse asymmetry leakage in $A_{PV} < 2\,\text{ppb}$

Ancillary Measurements: Transverse Asymmetry

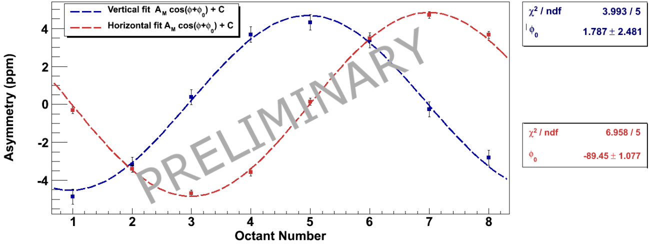

- Vertical polarization: cancellation with helicity reversal
- Horizontal polarization: 90° phase shift from vertical
- Shown asymmetries not corrected for backgrounds or polarization
- Preliminary transverse asymmetry: $B_n = -5.27 \pm 0.07(\text{stat}) \pm 0.14(\text{syst})$ ppm
- Transverse asymmetry leakage in $A_{PV} < 2$ ppb

Ancillary Measurements: Transverse Asymmetry

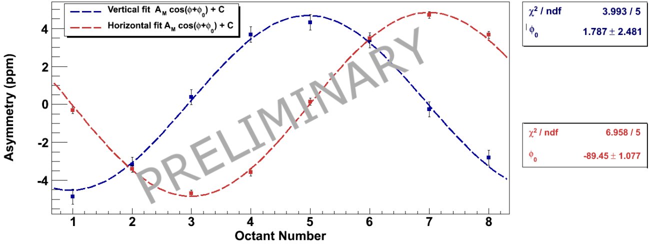

- Vertical polarization: cancellation with helicity reversal
- Horizontal polarization: 90° phase shift from vertical
- Shown asymmetries not corrected for backgrounds or polarization
- Preliminary transverse asymmetry:
  $B_n = -5.27 \pm 0.07(\text{stat}) \pm 0.14(\text{syst})\,\text{ppm}$
- Transverse asymmetry leakage in $A_{PV} < 2\,\text{ppb}$

Ancillary Measurements: Transverse Asymmetry

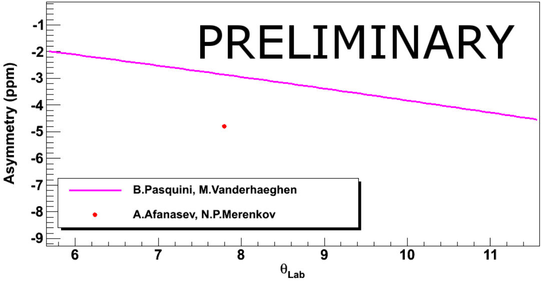

- Pasquini & Vanderhaeghen: proton and πN, resonance region with MAID, asymmetry dominated by inelastic contribution
- Afanasev & Merenkov: forward Compton amplitudes from real photo-production
- $E = 1.160\,\text{GeV}$, $\theta = 7.8^\circ$, $Q^2 = 0.026\,\text{GeV}^2$
- Other measurements: 0.877 GeV and 3.36 GeV, on Al and C

Ancillary Measurements: Transverse Asymmetry

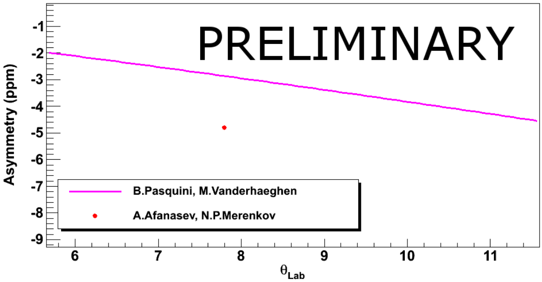

- Pasquini & Vanderhaeghen: proton and πN, resonance region with MAID, asymmetry dominated by inelastic contribution
- Afanasev & Merenkov: forward Compton amplitudes from real photo-production
- $E = 1.160\,\mathrm{GeV}$, $\theta = 7.8°$, $Q^2 = 0.026\,\mathrm{GeV}^2$
- Other measurements: 0.877 GeV and 3.36 GeV, on Al and C

Ancillary Measurements: Transverse Asymmetry

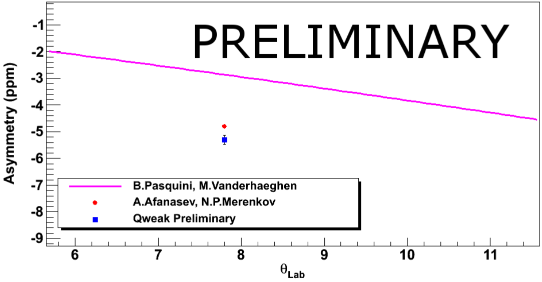

- Pasquini & Vanderhaeghen: proton and πN, resonance region with MAID, asymmetry dominated by inelastic contribution
- Afanasev & Merenkov: forward Compton amplitudes from real photo-production
- $E = 1.160\,\text{GeV}$, $\theta = 7.8^\circ$, $Q^2 = 0.026\,\text{GeV}^2$
- Other measurements: 0.877 GeV and 3.36 GeV, on Al and C

First Determination of the Weak Charge of the Proton

First results

- Publication in Phys. Rev. Lett. 111, 141803 (2013)
- Based on only 4% of the total data set: first experiment with direct access to proton's weak charge
- 25 times more data available: projected release in fall 2014

Global analysis method by Young, Roche, Carlini, Thomas

- Fit of parity-violating asymmetry data on H, D, ^{4}He, up to $Q^2 = 0.63\,\mathrm{GeV}^2$, and rotated to zero forward angle
- Free parameters were C_{1u}, C_{1d}, strange charge radius ρ_s and magnetic moment μ_s, and isoscalar axial form factor (zero at tree level)

Determination of the Weak Charge of the Proton

Reduced parity-violating asymmetry

$$\overline{A_{PV}} = \frac{A_{PV}}{A_0} = Q_W^p + Q^2 \cdot B(Q^2, \theta = 0) \quad \text{with} \quad A_0 = -\frac{G_F Q^2}{4\pi\alpha\sqrt{2}}$$

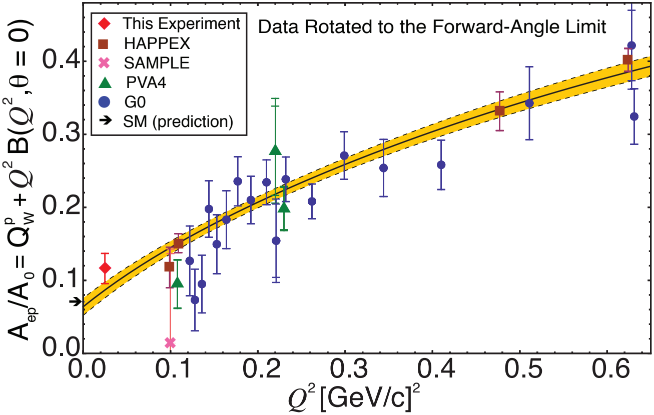

Section 9

Summary

Sensitivity to New Physics

Different experiments sensitive to different extensions

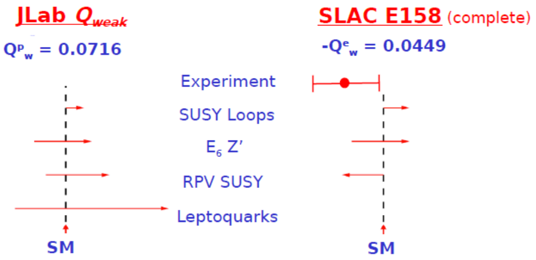

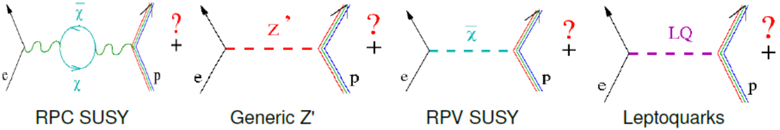

Data Quality: Understanding the Width

Asymmetry width

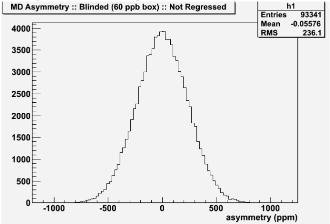

Battery width

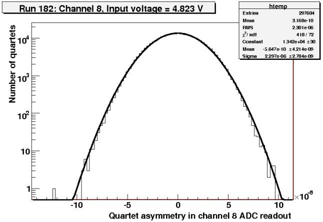

Measurement

- 240 Hz helicity quartets $(+--+$ or $-++-)$
- Uncertainty $= RMS/\sqrt{N}$
- 200 ppm in 4 milliseconds
- $<$ 1 ppm in 5 minutes

Asymmetry width

- Pure counting statistics $\approx$ 200 ppm
- $+$ detector resolution $\approx$ 90 ppm
- $+$ current monitor $\approx$ 50 ppm
- $+$ target boiling $\approx$ 57 ppm
- $=$ observed width $\approx$ 233 ppm

The Q_{Weak} Experiment: Tracking Mode

Horizontal drift chambers

- 32 wires in 0.5 m wide planes
- 12 planes per octant
- 2 instrumented octants
- Constructed at Va Tech

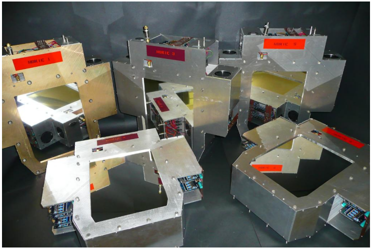

Vertical drift chambers

- 181 wires in 2 m long planes
- 4 planes per octant (65° tilt)
- 2 instrumented octants
- Constructed at W&M

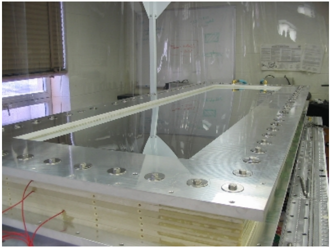

The Q_{Weak} Experiment: Tracking Mode

Horizontal drift chambers

- 32 wires in 0.5 m wide planes
- 12 planes per octant
- 2 instrumented octants
- Constructed at Va Tech

Vertical drift chambers

- 181 wires in 2 m long planes
- 4 planes per octant (65° tilt)
- 2 instrumented octants
- Constructed at W&M

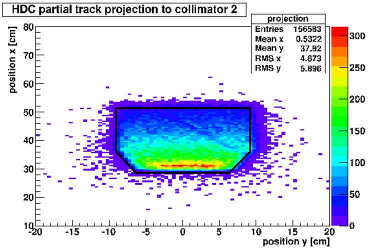

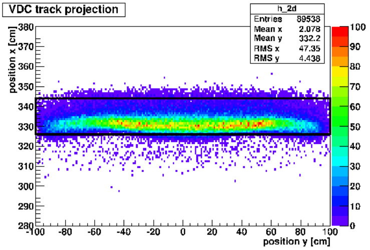

The Q_{Weak} Experiment: Tracking Mode

Reconstruction of angle θ (preliminary)

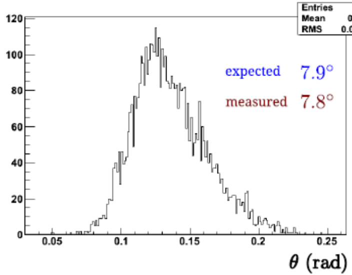

Reconstruction of momentum transfer Q^2 (preliminary)

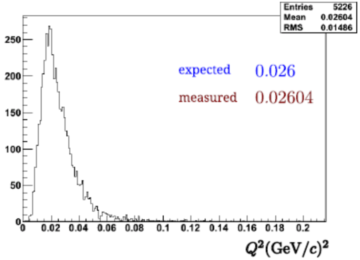

- Periodic tracking runs at 50 pA (HDC/VDC) to few nA (VDC)
- VDC track resolution of 250 μm meets design goal
- HDC track resolution of 350 μm (work ongoing)
- Required precision of 0.5% on value of Q^2 achievable

The Q_{Weak} Experiment: Tracking Mode

Simulation of electrons hitting main detector bar

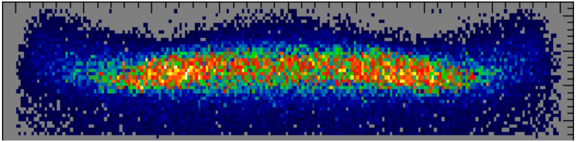

Projection of reconstructed tracks to detector bar

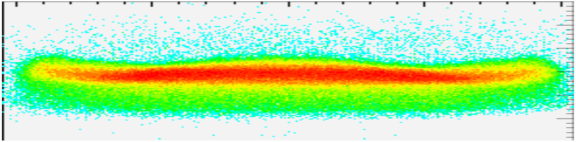

Focal plane scanner detector (1 cm square quartz)

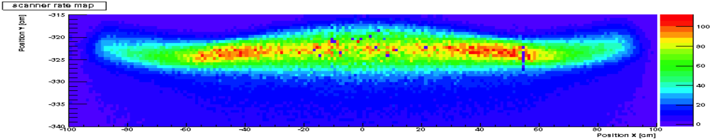

Data Quality: Helicity-Correlated Beam Properties

Natural beam motion

- Measured asymmetry correlated with beam position and angles
- False asymmetries
- Linear regression removes effect:
  $A_c = \sum_i \frac{\partial A}{\partial x_i} \Delta x_i$
  $i = x, y, x', y', E$

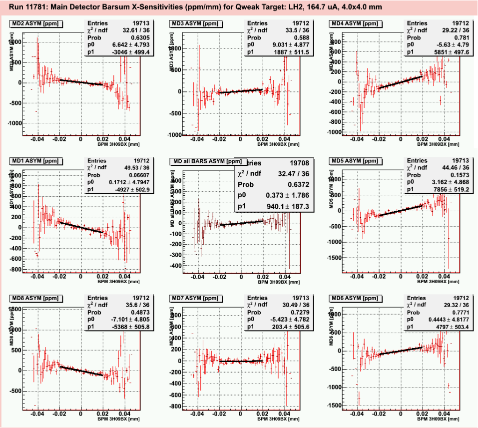

Data Quality: Helicity-Correlated Beam Properties

Driven beam motion

- Deliberate motion
- $i = x, y, x', y', E$

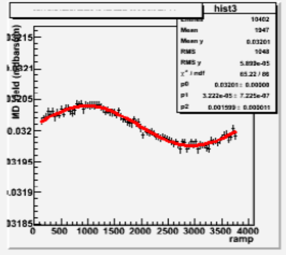

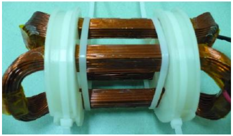

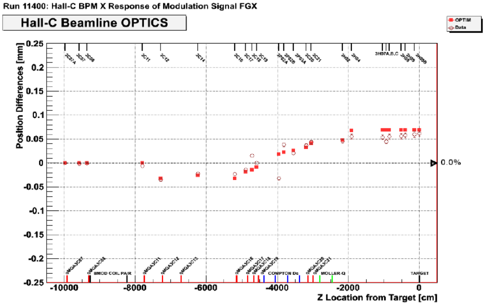

- Sensitivity slopes $\frac{\partial A}{\partial x_i}$ determined from natural beam motion or from beam modulation $\rightarrow$ results consistent between methods
- Actual regression corrections smaller than specifications

Sensitivity to New Physics

Lower bound on new physics (95% CL)

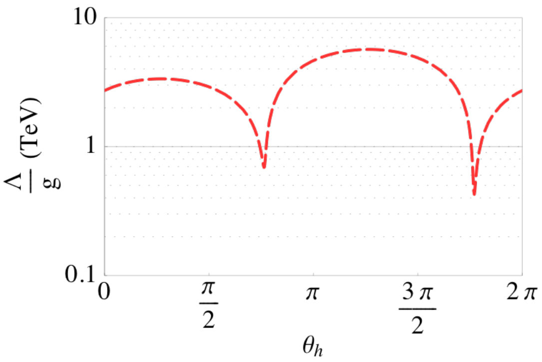

Figure: Young, Carlini, Thomas, Roche (2007)

Constraints from

- Atomic PV: $\frac{\Lambda}{g} > 0.4$ *TeV*
- PV electron scattering: $\frac{\Lambda}{g} > 0.9$ *TeV*

Projection Q_{Weak}

- $\frac{\Lambda}{g} > 2$ *TeV*
- 4% precision

Sensitivity to New Physics

Lower bound on new physics (95% CL)

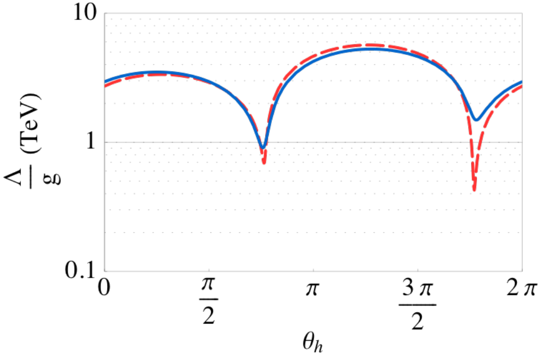

Figure: Young, Carlini, Thomas, Roche (2007)

Constraints from

- Atomic PV: $\frac{\Lambda}{g} > 0.4$ *TeV*
- PV electron scattering: $\frac{\Lambda}{g} > 0.9$ *TeV*

Projection Q_{Weak}

- $\frac{\Lambda}{g} > 2$ *TeV*
- 4% precision

Sensitivity to New Physics

Lower bound on new physics (95% CL)

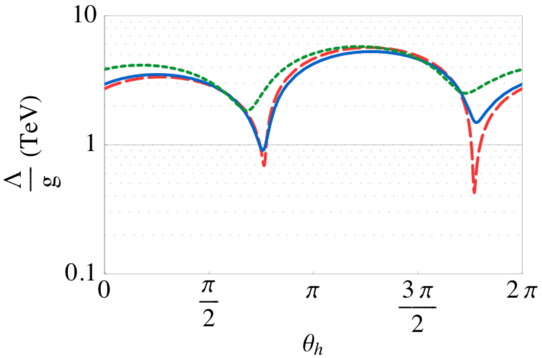

Figure: Young, Carlini, Thomas, Roche (2007)

Constraints from

- Atomic PV: $\frac{\Lambda}{g} > 0.4$ *TeV*
- PV electron scattering: $\frac{\Lambda}{g} > 0.9$ *TeV*

Projection Q_{Weak}

- $\frac{\Lambda}{g} > 2$ *TeV*
- 4% precision

Sensitivity to New Physics

Different experiments sensitive to different extensions

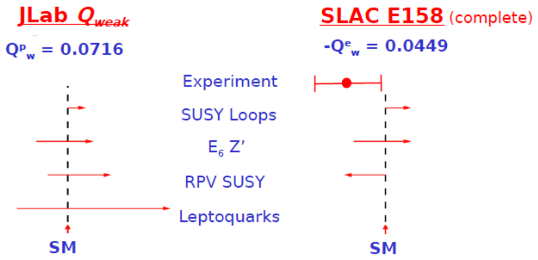

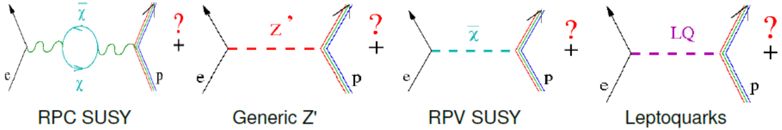

Parity-Violating Electron Scattering: Quark Couplings

Weak vector charge *uud*

$Q_W^p = -2(2C_{1u} + C_{1d})$

Early experiments

- SLAC and APV

Electron scattering

- HAPPEx, G0
- PVA4/Mainz
- SAMPLE/Bates

Q_{Weak} experiment

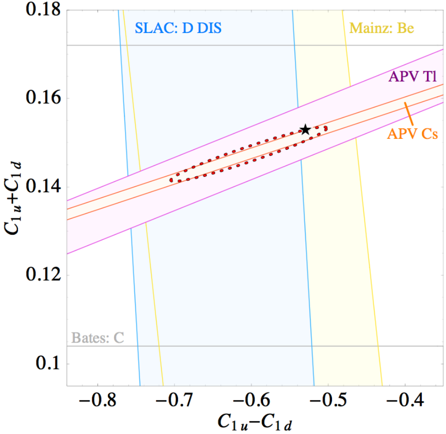

Figure: Young, Carlini, Thomas, Roche

Parity-Violating Electron Scattering: Quark Couplings

Weak vector charge *uud*

$Q_W^p = -2(2C_{1u} + C_{1d})$

Early experiments

- SLAC and APV

Electron scattering

- HAPPEx, G0
- PVA4/Mainz
- SAMPLE/Bates

Q_{Weak} experiment

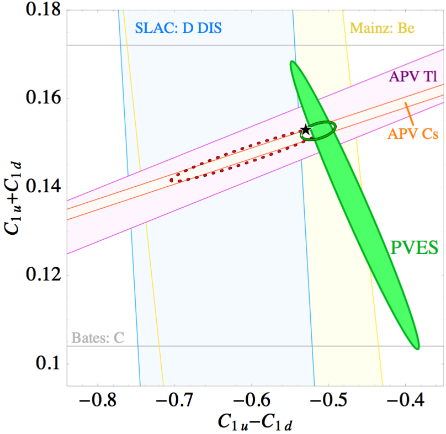

Figure: Young, Carlini, Thomas, Roche

Parity-Violating Electron Scattering: Quark Couplings

Weak vector charge *uud*

$Q_W^p = -2(2C_{1u} + C_{1d})$

Early experiments

- SLAC and APV

Electron scattering

- HAPPEx, G0
- PVA4/Mainz
- SAMPLE/Bates

Q_{Weak} experiment

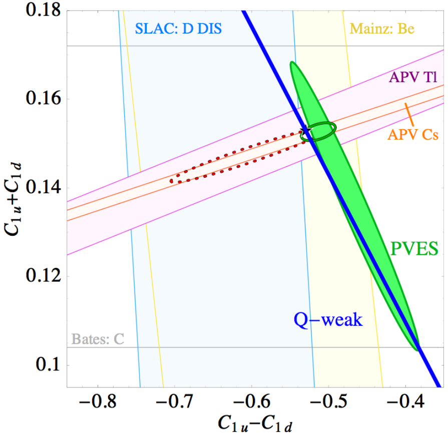

Figure: Young, Carlini, Thomas, Roche

Section 10

Precision Polarimetry with Atomic Hydrogen

Precision Electroweak Experiments: JLab 12 GeV

MOLLER Experiment

Source	ΔA_{PV}
Mom. transfer Q^2	0.5%
Beam polarization	0.4%
2^{nd} order beam	0.4%
Inelastic *ep*	0.4%
Elastic *ep*	0.3%

SoLID PV-DIS Experiment

Source	ΔA_{PV}
Beam polarization	0.4%
Rad. corrections	0.3%
Mom. transfer Q^2	0.5%
Inelastic *ep*	0.2%
Statistics	0.3%

Precision beam polarimetry is crucial to these experiments.

Precision Electroweak Experiments: Polarimetry

Compton Polarimetry

- $\vec{e}\vec{\gamma} \to e\gamma$ (polarized laser)
- Detection e and/or γ
- Only when beam energy above few hundred MeV
- High photon polarization but low asymmetry
- Total systematics $\sim 1\%$
  - laser polarization
  - detector linearity

Møller Polarimetry

- $\vec{e}\vec{e} \to ee$ (magnetized Fe)
- Low current because temperature induces demagnetization
- High asymmetry but low target polarization
- Levchuk effect: scattering off internal shell electrons
- Intermittent measurements at different beam conditions
- Total systematics $\sim 1\%$

Atomic Hydrogen Polarimetry

Møller polarimetry

- 300 mK cold atomic H
- 8 T solenoid trap
- $3 \cdot 10^{16}$ atoms/cm^2
- $3 \cdot 10^{15-17}$ atoms/cm^3
- 100% polarization of e in the atomic hydrogen

Advantages

- High beam currents
- No Levchuk effect
- Non-invasive, continuous

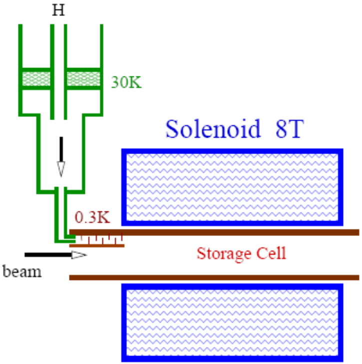

Reference: E. Chudakov, V. Luppov, IEEE Trans. on Nucl. Sc. 51, 1533 (2004).

Atomic Hydrogen Polarimetry: 100% e Polarization

Hyperfine Splitting in Magnetic Field

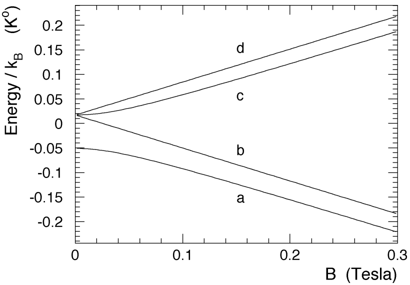

- Force $\vec{\nabla}(-\vec{\mu} \cdot \vec{B})$ will pull $|a\rangle$ and $|b\rangle$ into field

- Energy splitting of $\Delta E = 2\mu B$: $\uparrow / \downarrow = \exp(-\Delta E/kT) \approx 10^{-14}$
- Low energy states with $|s_e s_p\rangle$:
  - $|d\rangle = |\uparrow\Uparrow\rangle$
  - $|c\rangle = \cos\theta\,|\uparrow\Downarrow\rangle + \sin\theta\,|\downarrow\Uparrow\rangle$
  - $|b\rangle = |\downarrow\Downarrow\rangle$
  - $|a\rangle = \cos\theta\,|\downarrow\Uparrow\rangle - \sin\theta\,|\uparrow\Downarrow\rangle$
  - with $\sin\theta \approx 0.00035$
- $P_e(\downarrow) \approx 1$ with only 10^5 dilution from $|\uparrow\Downarrow\rangle$ in $|a\rangle$ at $B = 8\,\mathrm{T}$
- $P_p(\Uparrow) \approx 0.06$ because 53% $|a\rangle$ and 47% $|b\rangle$

Atomic Hydrogen Polarimetry: Expected Contaminations

Without beam

- Recombined molecular hydrogen suppressed by coating of cell with superfluid He, $\sim 10^{-5}$
- Residual gasses, can be measured with beam to $< 0.1\%$

With $100\,\mu$A beam

- 497 MHz RF depolarization for 200 GHz $|a\rangle \rightarrow |c\rangle$ transition, tuning of field to avoid resonances, uncertainty $\sim 2 \cdot 10^{-4}$
- Ion-electron contamination: builds up at 20%/s in beam region, cleaning with $\vec{E}$ field of $\sim 1\,$V/cm, uncertainty $\sim 10^{-5}$

Atomic Hydrogen Polarimetry: Projected Uncertainties

Projected Systematic Uncertainties ΔP_e in Møller polarimetry

Source	Fe-foil	Hydrogen
Target polarization	0.63%	0.01%
Analyzing power	0.30%	0.10%
Levchuk effect	0.50%	0.00%
Deadtime	0.30%	0.10%
Background	0.30%	0.10%
Other	0.30%	0.00%
Unknown unknowns	0.00%	0.30%(?)
Total	1.0%	0.35%

Atomic Hydrogen Polarimetry: Collaboration with Mainz

P2 Experiment in Mainz: Weak Charge of the Proton

- "Q_{Weak} experiment" with improved statistical precision
- Dedicated 200 MeV accelerator MESA under construction
- Required precision of electron beam polarimetry $< 0.5\%$
- Strong motivation for collaboration on a short timescale (installation in 2017)

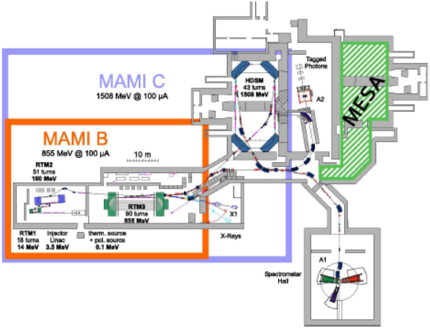

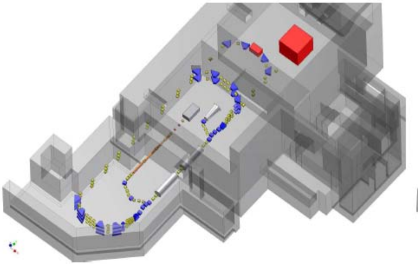

Ancillary Measurements: Background Processes

Aluminum asymmetry (preliminary)

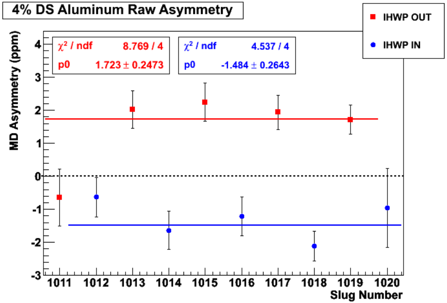

- Asymmetry consistent with order of magnitude expected

- Asymmetry: few ppm
- Dilution f of 3%
- Correction $\approx$ 20%

Dilution measurement (preliminary)

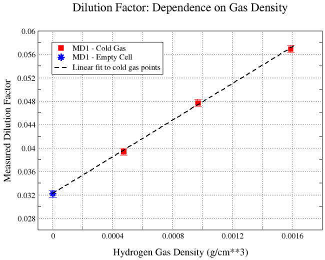

Radiative Corrections

Modified expression, $Q_W^p = 1 - 4\sin^2\theta_W$ only at tree level

- $Q_W^p = (\rho_{NC} + \Delta_e)(1 - 4\sin^2\theta_W(0) + \Delta'_e) + B_{WW} + B_{ZZ} + B_{\gamma Z}$
- $\Delta\sin^2\theta_W(M_Z)$, WW, ZZ box diagrams: uncertainty small
- γZ box: 8% correction with $\approx$ 1% uncertainty

Corrections to $Q_W^p \approx 0.07$

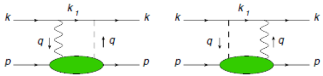

Source	Q^p_{Weak} Uncertainty
$\Delta\sin\theta_W(M_Z)$	±0.0006
$Z\gamma$ box	±0.0005
$\Delta\sin\theta_W(Q)_{hadronic}$	±0.0003
WW, ZZ box - pQCD	±0.0001
Charge symmetry	0
Total	±0.0008

Erler et al., PRD 68(2003)016006.

- Verification in "DIS" region, calculation by Melnitchouk

Radiative Corrections

Modified expression, $Q_W^p = 1 - 4\sin^2\theta_W$ only at tree level

- $Q_W^p = (\rho_{NC} + \Delta_e)(1 - 4\sin^2\theta_W(0) + \Delta_e') + B_{WW} + B_{ZZ} + B_{\gamma Z}$
- $\Delta \sin^2\theta_W(M_Z)$, WW, ZZ box diagrams: uncertainty small
- γZ box: 8% correction with $\approx$ 1% uncertainty

Corrections to $Q_W^p \approx 0.07$

Source	Q^p_{Weak} Uncertainty
$\Delta \sin\theta_W (M_Z)$	±0.0006
$Z\gamma$ box	±0.0005
$\Delta \sin\theta_W (Q)_{hadronic}$	±0.0003
WW, ZZ box - pQCD	±0.0001
Charge symmetry	0
Total	±0.0008

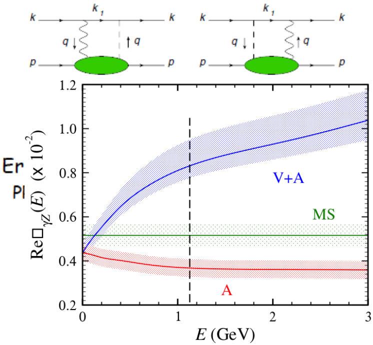

- Verification in "DIS" region, calculation by Melnitchouk

Radiative Corrections

Modified expression, $Q_W^p = 1 - 4\sin^2\theta_W$ only at tree level

- $Q_W^p = (\rho_{NC} + \Delta_e)(1 - 4\sin^2\theta_W(0) + \Delta'_e) + B_{WW} + B_{ZZ} + B_{\gamma Z}$
- $\Delta\sin^2\theta_W(M_Z)$, WW, ZZ box diagrams: uncertainty small
- γZ box: 8% correction with $\approx$ 1% uncertainty

Corrections to $Q_W^p \approx 0.07$

Source	Q^p_{Weak} Uncertainty
$\Delta\sin\theta_W(M_Z)$	±0.0006
$Z\gamma$ box	±0.0005
$\Delta\sin\theta_W(Q)_{hadronic}$	±0.0003
WW, ZZ box - pQCD	±0.0001
Charge symmetry	0
Total	±0.0008

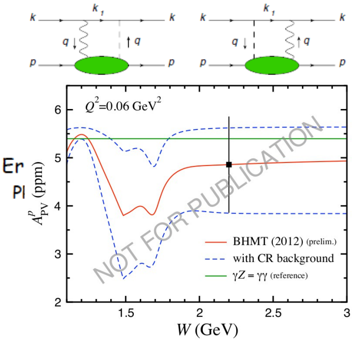

- Verification in "DIS" region, calculation by Melnitchouk

Section 11

The Q_{Weak} Experiment

The Q_{Weak} Experiment: Main Detector

Event mode characterization

- Larger signal in + or - end depending on proximity
- Number of photo-electrons ≈ 85 per track

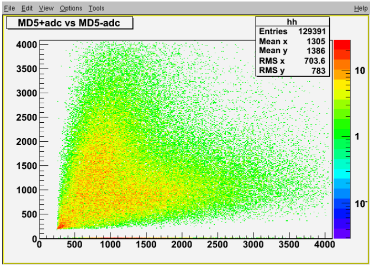

Integrating data chain noise

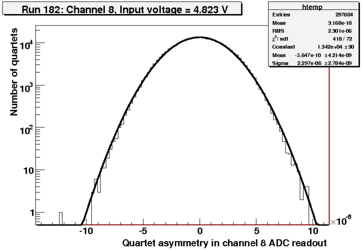

- Current source (battery)
  - Width ≈ 2.3 ppm
- Actual data with beam
  - Width ≈ 240 ppm
- Not limited by electronic noise

The Q_{Weak} Experiment: Main Detector

Event mode characterization

- Larger signal in + or - end depending on proximity
- Number of photo-electrons $\approx$ 85 per track

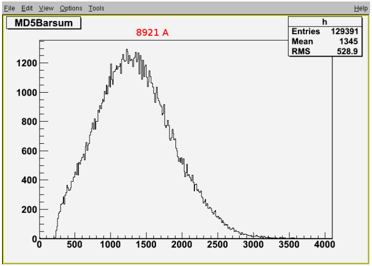

Integrating data chain noise

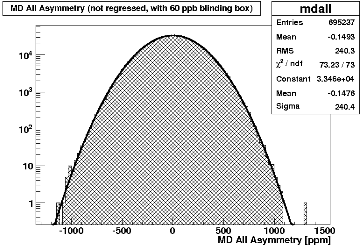

- Current source (battery)
  - Width $\approx$ 2.3 ppm
- Actual data with beam
  - Width $\approx$ 240 ppm
- Not limited by electronic noise

The Q_{Weak} Experiment: Systematic Uncertainties

Projected uncertainties on A_{meas} and Q_W^p

Source of uncertainty	Contribution to $\Delta A_{meas}/A_{meas}$	Contribution to $\Delta Q_W^p/Q_W^p$
Statistics	2.1%	3.2%
Hadronic structure	–	1.5%
Beam polarimetry	1.0%	1.5%
Measurement Q^2	0.5%	1.0%
Backgrounds	0.5%	0.7%
Helicity-correlated beam properties	0.5%	0.7%
Total	2.5%	4.1%

Parity-Violating Electron Scattering

Reduced parity-violating asymmetry

$$\overline{A_{PV}}(p) = A_{PV}(p) \cdot \frac{4\pi\alpha\sqrt{2}}{-G_F Q^2} \xrightarrow{Q^2 \to 0} Q_W^p + Q^2 \cdot B(Q^2)$$

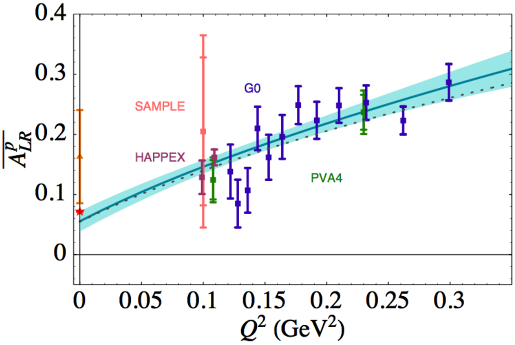

At $Q^2 = 0$

- PDG
- SM

Q_{Weak} Exp

- $Q^2 = 0.026\,\text{GeV}^2$

Figure: Young, Carlini, Thomas, Roche (2007)

Divide out leading
Q^2 dependence:

$$\overline{A^p_{LR}} \simeq Q^p_{weak} + B(Q^2)Q^2 + \ldots$$

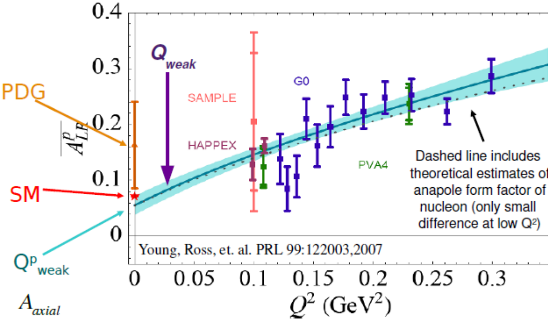

$$A = A_{Q^p_W} + A_{hadronic} + A_{axial}$$

$$= -0.17 \text{ ppm} - 0.07 \text{ ppm} - 0.01 \text{ ppm}$$

hadronic:
(31% of asymmetry)
contains $G^{\gamma}_{E,M}$ $G^{Z}_{E,M}$
Constrained by
HAPPEX, G^0, MAMI PVA4

axial:
(4% of asymmetry)
contains G^e_A
large electroweak
radiative corrections
Constrained by G^0
and SAMPLE

Parity-Violating Electron Scattering: $\sin^2\theta_W$

Running of $\sin^2\theta_W$
$(Q_W^p = 1 - 4\sin^2\theta_W)$

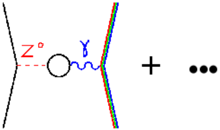

- Higher order loop diagrams
- $\sin^2\theta_W$ varies with Q^2

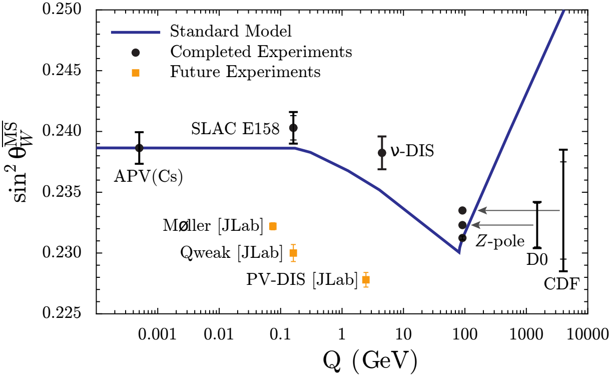

Section 12

Radiative Corrections

γZ Box Corrections near 1.16 GeV

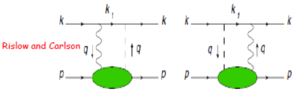

In 2009, Gorchtein and Horowitz showed the vector hadronic contribution to be significant and energy dependent.

This soon led to more refined calculations with corrections of ~8% and error bars ranging from ±1.1% to ±2.8%.

It will probably also spark a refit of the global PVES database used to constrain G_E^s, G_M^s, G_A.

PV Amplitude	Authors	Correction* @ E=1.165 (GeV)
$A^e \times V^p$ (vanishes as E→0)	GH	0.0026+-0.0026**
	SBMT	0.0047 $^{+0.0011}_{-0.0004}$
	RC	0.0057±0.0009
	GHR-M	0.0054±0.0020
$V^e \times A^p$ (finite as E→0)	MS (as updated by EKR-M)	0.0052±0.0005***
	BMT	0.0037±0.0004

*Does not include a small contribution from the elastic.
** 5.7%×Q_w^p(LO) = 0.0026. Q_w^p(LO) = 0.04532.
***Included in Q_w^p. For reference, Q_w^p =0.0713(8).

BMT and references
(V and A are hadronic couplings)

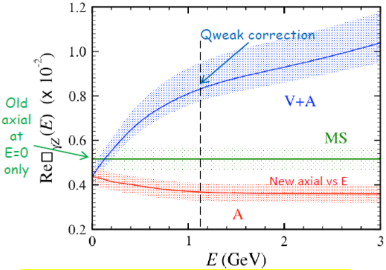

Forthcoming axial results for Q_w^n have the potential to impact the interpretation of Cs APV.

1

γZ Box Corrections near 1.16 GeV
A Partial Bibliography

PV Amplitude	Authors	Reference
$A^e x V^p$ (vanishes as E→0)	GH	Gorchtein & Horowitz, PRL **102**, 091806 (2009)
	SBMT	Sibirtsev, Blunden, Melnitchouk, and Thomas, PRD **82**, 013011 (2010)
	RC	Rislow & Carlson, PRD **83**, 113007 (2011)
	GHR-M	Gorchtein, Horowitz, and Ramsey-Musolf, PRC **84**, 015502 (2011)
$V^e x A^p$ (finite as E→0)	MS	Marciano and Sirlin, PRD **27**, 552 (1983), PRD **29**, 75 (1984)
	EKR-M	Erler, Kurylov, and Ramsey-Musolf, PRD **68**, 016006 (2003)
	BMT	Blunden, Melnitchouk, and Thomas, PRL **107**, 081801 (2011)

The Q_{Weak} Experiment: Toroidal Magnet (QTOR)

QTOR installed in Hall C

- Full assembly and power supply tests
- Mapped at half field, within tolerances

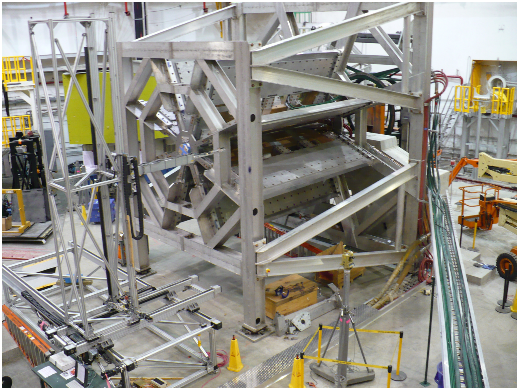

QTOR properties

- Warm coils
- 10000 A
- 6 m high

Large coils aligned to 1 mm

At MIT/Bates

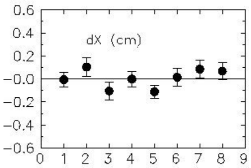

The Q_{Weak} Experiment: Main Detector

Low noise electronics

- Event rate: 800 MHz/PMT
- Asymmetry of only 0.2 ppm
- Low noise electronics (custom design, TRIUMF)

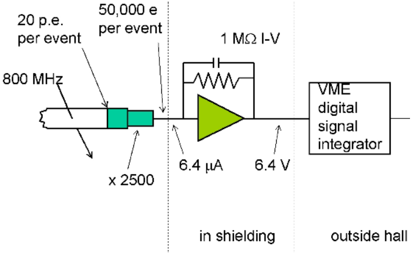

I-V Preamplifier

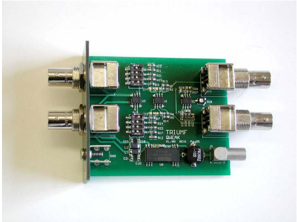

18-bit 500 kHz sampling ADC

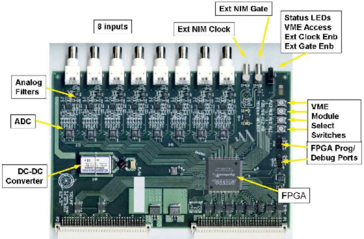

Delivered, tested: noise is 3 times lower than counting statistics

The Q_{Weak} Experiment: Systematic Uncertainties

Reminder: weak vector charges

- Proton weak charge $Q_W^p \approx -0.072$
- Neutron weak charge $Q_W^n = -1$

Sources of neutron scattering

- Al target windows
- Secondary collimator events
- Small number of events, but huge false PV asymmetry

Al target windows

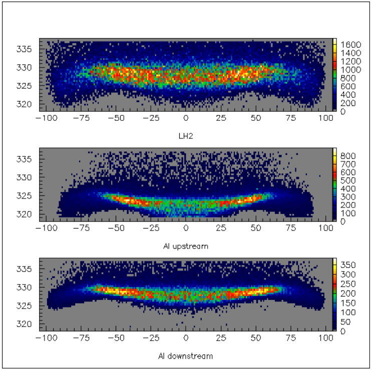

The Q_{Weak} Experiment: Systematic Uncertainties

Largest projected uncertainties on Q_W^p

- Total uncertainty on Q_W^p: 4.1%
- Statistical uncertainty: 3.2%
- Hadronic structure: 1.5%
- Beam polarimetry: 1.5%
- Measurement of Q^2: 1.0%
- Background events: 0.7%
- Helicity-correlated beam properties: 0.7%

Responsibilities of MIT group

- Track reconstruction/momentum determination software
- Construction of Compton polarimeter

The Q_{Weak} Experiment: Systematic Uncertainties

Largest projected uncertainties on Q_W^p

- Total uncertainty on Q_W^p: 4.1%
- Statistical uncertainty: 3.2%
- Hadronic structure: 1.5%
- Beam polarimetry: 1.5%
- Measurement of Q^2: 1.0%
- Background events: 0.7%
- Helicity-correlated beam properties: 0.7%

Responsibilities of MIT group

- Track reconstruction/momentum determination software
- Construction of Compton polarimeter

The Q_{Weak} Experiment: Systematic Uncertainties

Largest projected uncertainties on Q_W^p

- Total uncertainty on Q_W^p: 4.1%
- Statistical uncertainty: 3.2%
- Hadronic structure: 1.5%
- Beam polarimetry: 1.5%
- Measurement of Q^2: 1.0%
- Background events: 0.7%
- Helicity-correlated beam properties: 0.7%

Responsibilities of MIT group

- Track reconstruction/momentum determination software
- Construction of Compton polarimeter

The Q_{Weak} Experiment: Systematic Uncertainties

Largest projected uncertainties on Q_W^p

- Total uncertainty on Q_W^p: 4.1%
- Statistical uncertainty: 3.2%
- Hadronic structure: 1.5%
- Beam polarimetry: 1.5%
- Measurement of Q^2: 1.0%
- Background events: 0.7%
- Helicity-correlated beam properties: 0.7%

Responsibilities of MIT group

- Track reconstruction/momentum determination software
- Construction of Compton polarimeter

The Q_{Weak} Experiment: Tracking Mode

Gas-electron multiplier (GEM)

- Very close to target, very high dose
- GEMs have high radiation hardness
- Several days of radcon cool-down in GEM bunker
- Remotely controlled rotator mounted on collimator

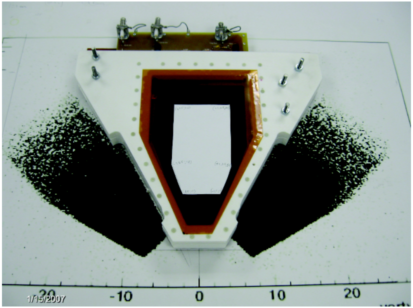

The Q_{Weak} Experiment: Tracking Mode

Horizontal drift chambers (HDC)

- 12 planes per octant
- u, v, x, u, v, x planes per assembly

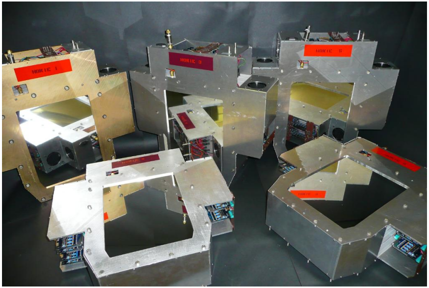

- $4 + 1$ constructed, tested
- Residuals from cosmic events
- Ready for installation

HDC rotator system

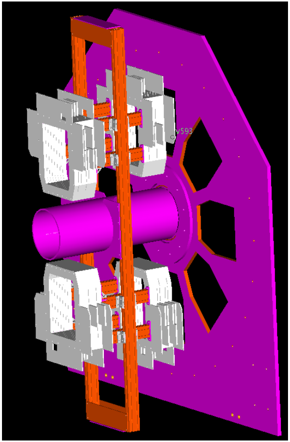

The Q_{Weak} Experiment: Tracking Mode

Vertical drift chambers (VDC)

- 181 wires in 2 m wide planes
- u, v, u, v planes per assembly
- Multiplexed read-out on delay lines

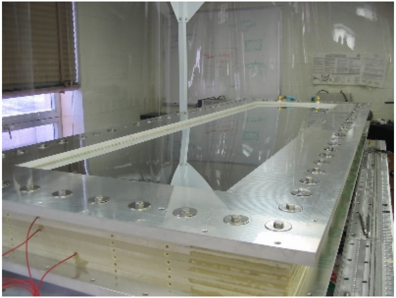

Principle of operation

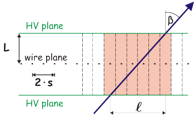

VDC rotator system

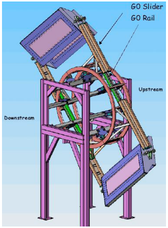

Electroweak Interaction: Running of $\sin^2\theta_W$

Atomic parity-violation on ^{133}Cs

- New calculation in many-body atomic theory
- Porsev, Beloy, Derevianko; arXiv:0902.0335 [hep-ph]
- Experiment: $Q_W(^{133}\text{Cs}) = -73.25 \pm 0.29 \pm 0.20$
- Standard Model: $Q_W(^{133}\text{Cs}) = -73.16 \pm 0.03$

NuTeV anomaly explained

- Originally, $3\,\sigma$ deviation from Standard Model
- Erler, Langacker: strange quark PDFs
- Londergan, Thomas: charge symmetry violation, $m_u \neq m_d$
- Cloet, Bentz, Thomas: in-medium modifications to PDFs, isovector EMC-type effect
- Entire anomaly accounted for (everybody stops looking...)

Electroweak Interaction

Running of $\sin^2\theta_W$

- Higher order loop diagrams
- $\sin^2\theta_W$ varies with Q^2

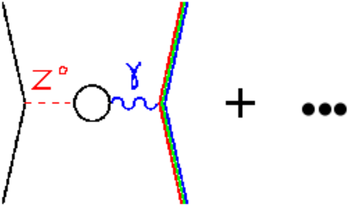

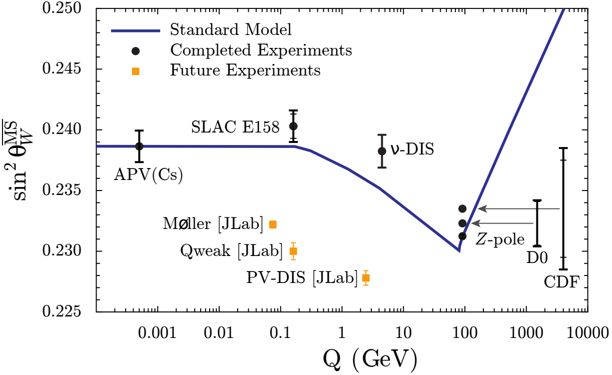

Electroweak Interaction

Running of $\sin^2\theta_W$

- Higher order loop diagrams
- $\sin^2\theta_W$ varies with Q^2

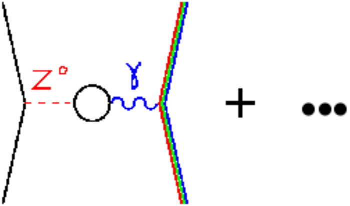

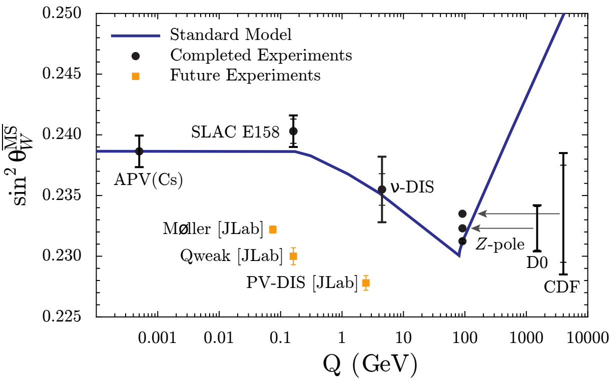

Sensitivity to New Physics

New physics

- Consider effective contact interaction
- Coupling constant g, mass scale Λ
- Effective charges h_V^u and h_V^d

Effective Lagrangian

$$\begin{aligned}\mathcal{L}_{e-q}^{PV} &= \mathcal{L}_{SM}^{PV} + \mathcal{L}_{New}^{PV} \\ &= -\frac{G_F}{\sqrt{2}}\bar{e}\gamma_\mu\gamma_5 e \sum_q C_{1q}\bar{q}\gamma^\mu q + \frac{g^2}{4\Lambda^2}\bar{e}\gamma_\mu\gamma_5 e \sum_q h_q^V \bar{q}\gamma^\mu q\end{aligned}$$

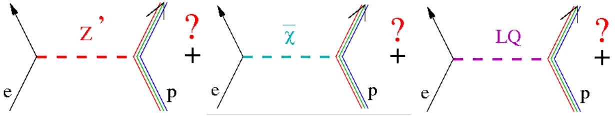

Erler *et al.*, PRD 68, 016006 (2003)

Other Experiments